

Characterization of uremic toxin transport by organic anion transporters in the kidney

TSUNEO DEGUCHI, HIROYUKI KUSUHARA, AKIRA TAKADATE, HITOSHI ENDOU, MASAKI OTAGIRI, and YUICHI SUGIYAMA

Graduate School of Pharmaceutical Sciences, University of Tokyo, Tokyo, Japan; Department of Biopharmaceutics, Graduate School of Pharmaceutical Sciences, Kumamoto University, Kumamoto, Japan; Daiichi College of Pharmaceutical Sciences, Fukuoka, Japan; Department of Pharmacology and Toxicology, Kyorin University School of Medicine, Tokyo, Japan

Characterization of uremic toxin transport by organic anion transporters in the kidney.

Background. Harmful uremic toxins, such as indoxyl sulfate (IS), 3-carboxy-4-methyl-5-propyl-2-furanpropionate (CMPF), indoleacetate (IA), and hippurate (HA), accumulate to a high degree in uremic plasma. IS has been shown to be a substrate of rat organic anion transporter 1 (rOat1) and rOat3. However, the contribution of rOat1 and rOat3 to the renal uptake transport process of IS and other uremic toxins in the kidney remains unknown.

Methods. The cellular uptake of uremic toxins was determined using stable transfectants of rOat1/hOAT1 and rOat3/hOAT3 cells. Also, the uptake of uremic toxins by rat kidney slices was characterized to evaluate the contribution of rOat1 and rOat3 to the total uptake by kidney slices using inhibitors of rOat1 (*p*-aminohippurate) and rOat3 (pravastatin and benzylpenicillin).

Results. Saturable uptake of IS, CMPF, IA, and HA by rOat1 was observed with K_m values of 18, 154, 47, and 28 $\mu\text{mol/L}$, respectively, whereas significant uptake of IS and CMPF, but not of IA or HA, was observed in rOat3-expressing cells with K_m values of 174 and 11 $\mu\text{mol/L}$, respectively. Similar parameters were obtained for human OAT1 and OAT3. Kinetic analysis of the IS uptake by kidney slices revealed involvement of two saturable components with K_{m1} (24 $\mu\text{mol/L}$) and K_{m2} (196 $\mu\text{mol/L}$) values that were comparable with those of rOat1 and rOat3. The K_m value of CMPF uptake by kidney slices (22 $\mu\text{mol/L}$) was comparable with that of rOat3, while the corresponding values of IA and HA (42 and 33 $\mu\text{mol/L}$, respectively) were similar to those of rOat1. PAH preferentially inhibited the uptake of IA and HA by kidney slices, while pravastatin and benzylpenicillin preferentially inhibited the uptake of CMPF. The effect of these inhibitors on the uptake of IS by kidney slices was partial.

Conclusion. rOat1/hOAT1 and rOat3/hOAT3 play major roles in the renal uptake of uremic toxins on the basolateral membrane of the proximal tubules. Both OAT1 and OAT3 contribute almost equally to the renal uptake of IS. OAT3 mainly

accounts for CMPF uptake by the kidney, while OAT1 mainly accounts for IA and HA uptake.

Uremic syndrome is a complex form of organ dysfunction, which causes the retention of waste products that, under normal condition, should be eliminated from the body by the kidneys [1]. Organic anions, such as indoxyl sulfate (IS), 3-carboxy-4-methyl-5-propyl-2-furanpropionate (CMPF), indoleacetate (IA) and hippurate (HA), derived from dietary protein, are mainly excreted into the urine, but they accumulate to a high degree in uremic plasma [2]. These organic anions have been proposed to cause uremic syndrome, including defective protein binding of drugs, irregularities in thyroid function, inhibition of active tubular secretion, neurologic symptoms, inhibition of drug metabolism in the liver, and stimulation of ammoniogenesis [3, 4]. Thus, these compounds have been referred to as “uremic toxins.” In particular, it has been proposed that the increased serum level of uremic toxins including IS may accelerate the deterioration of renal function in chronic renal failure [5]. In fact, administration of AST-120, an oral absorbent, decreased the serum and urinary concentrations of IS and prevented the progression of renal dysfunction by reducing the gene expression, such as transforming growth factor- β 1 (TGF- β 1), tissue inhibitor of metalloproteinase-1 (TIMP-1), and pro- α 1(I) collagen, in the kidney [6].

In renal tubules, membrane transport systems mediate the tubular secretion of endogenous and exogenous organic anions, such as various drugs, toxins, and endogenous metabolites. Rat organic anion transporter 1 (rOat1; *Slc22a6*), of which *p*-aminohippurate (PAH) is a typical substrate, was isolated from rat kidney as the classic renal organic anion transporter [7]. rOat1 is expressed predominantly in the kidney and is localized on the basolateral membrane of the middle proximal tubules (S2) [8]. rOat1 has broad substrate specificity and accepts a

Key words: uremic toxin, organic anion transporter.

Received for publication May 6, 2003
and in revised form July 22, 2003
Accepted for publication August 6, 2003

© 2004 by the International Society of Nephrology

variety of drugs, such as nonsteroidal anti-inflammatory agents, β -lactam antibiotics, methotrexate, and antiviral drugs and various endogenous organic anions, such as cyclic nucleotides, prostaglandins, dicarboxylates, and folate [9]. Subsequently, two isoforms, referred to as rOat2 (*Slc22a7*) and rOat3 (*Slc22a8*), were identified in rats [10, 11]. Northern blot analyses indicated that rOat2 is expressed abundantly in the liver and female kidney but only weakly in the male kidney [10, 12], while rOat3 is expressed in the male liver, kidney, brain, and only weakly in the eye [11]. rOat3 in the kidney is located on the basolateral membrane in all the segments (S1, S2, and S3) of the proximal tubules [13, 14]. Functional characterization shows that substrates of rOat3 include organic anions, such as estrone sulfate, pravastatin, benzylpenicillin (PCG), 17β -estradiol-D- 17β -glucuronide, ochratoxin A, PAH, and an organic cation, cimetidine [11, 14, 15]. The contribution of rOat1 and rOat3 to the renal uptake of organic anions has been evaluated in kidney slices, and it has been proposed that rOat1 is mainly responsible for the renal uptake of hydrophilic and small molecules, while rOat3 is responsible for the renal uptake of more bulky organic anions [14, 16]. Human OAT1 (hOAT1) and human OAT3 (hOAT3) are also predominantly expressed in the kidney and are coexpressed on the basolateral membrane in some part of the proximal tubules [17–19]. Based on transport studies in rats, it has been considered that hOAT1 and hOAT3 play a predominant role in the transport of organic anions across the basolateral membrane of human proximal tubules.

IS, CMPF, and HA produce significant inhibition of PAH transport in the kidney [2, 20, 21], suggesting that these compounds are transported by the organic anion transport system. Previous transport studies using expression systems have revealed that both rOat1 and rOat3 accept IS as a substrate [22, 23]. hOAT1 accepts IS and IA as a substrate [24], and IS is a substrate of hOAT3 and hOAT4 [25]. CMPF and HA have inhibitory effects on the renal uptake of IS in the *in vivo* tissue-sampling single-injection technique [i.e. the kidney uptake index (KUI) method] [22]. Moreover, HA significantly inhibited PAH transport by hOAT1-expressing cells [24]. Therefore, these uremic toxins have been suggested to be substrates of rOats/hOATs [2, 22, 24]. However, limited information is available concerning the contribution by rOat1 and rOat3 to the total renal uptake of uremic toxins in the kidney. It is important to identify the organic anion transporter responsible for the renal uptake of uremic toxins because inhibition or malfunction of the organic anion transporter will cause their serum accumulation. Furthermore, accumulation of uremic toxins in the circulating blood may lead to inhibition of the membrane transport of other exogenous and endogenous organic anions.

The purpose of the present study was to investigate the contribution of rOat1 and rOat3 to the renal uptake of uremic toxins (IS, CMPF, IA, and HA). Transport studies using cDNA-transfected cells revealed that rOat1/hOAT1 accepts all uremic toxins examined in this study as substrates, while rOat3/hOAT3 accepts only IS and CMPF. The uptake of uremic toxins was determined in kidney slices, and the effect of inhibitors relatively selective for rOat1 and rOat3 for their uptake was examined. Furthermore, kinetic parameters were compared between rat and human rOats/hOATs.

METHODS

Materials

CMPF was synthesized as previously described [26]. [^3H]IS (6.5 Ci/mmol) and [^3H]CMPF were synthesized and purified by Perkin Elmer Life Sciences (Boston, MA, USA). [^3H]IA (26.0 Ci/mmol) and [^3H]PCG (19.0 Ci/mmol) were obtained from Amersham Pharmacia Biotech (Little Chalfont, Buckinghamshire, UK). [^{14}C]HA (55 mCi/mmol) was purchased from American Radiolabeled Chemicals (St. Louis, MO, USA). [^3H]PAH (4.08 Ci/mmol) and [^{14}C]mannitol (51 mCi/mmol) were purchased from Perkin Elmer Life Sciences. Unlabeled IS, IA, and PAH were purchased from Sigma, and unlabeled HA, PCG, dibromosulfophthalein (DBSP) from Wako Pure Chemical Industries (Osaka, Japan). Unlabeled pravastatin was kindly donated by Sankyo (Tokyo, Japan). All other chemicals were of analytical grade and commercially available.

Cell culture

rOat1- and rOat3-expressing pig kidney epithelial cell line (LLC-PK1) cells were established as we described previously [15]. LLC-PK1 cells were grown on the bottom of a dish in M199 (Medium 199; Invitrogen, Carlsbad, CA, USA) supplemented with 10% fetal bovine serum, penicillin (100 U/mL), streptomycin (100 $\mu\text{g}/\text{mL}$), and G418 (400 $\mu\text{g}/\text{mL}$) (Geneticin; Invitrogen) at 37°C with 5% CO_2 and 95% humidity.

Stable transfectants of hOAT1 and hOAT3 were established using HEK293 cells as host. Briefly, full-length hOAT1 [17] was subcloned into the pcDNA3.1 vector (Invitrogen) and full-length hOAT3 [18] was subcloned into the pIRES2-EGFP vector (Clontech, Palo Alto, CA, USA). This construct of hOAT1 was introduced into HEK293 cells by lipofection with FuGENE 6 (Roche Diagnostics, Basel, Switzerland), and that of hOAT3 was introduced into HEK293 cells by lipofection with LipofectAMINE (Invitrogen) according to the manufacturer's protocols, and stable transfected cells were selected by adding G418 to the culture medium. Two weeks after transfection, positive clones were selected

by their transport activity for typical substrates (PAH for hOAT1 [17]; estrone sulfate and PCG for hOAT3 [18]). HEK293 cells were grown on the bottom of a dish in Dulbecco's modified Eagle's medium (Invitrogen) supplemented with 10% fetal bovine serum, penicillin (100 U/mL), streptomycin (100 µg/mL), and G418 (400 µg/mL) at 37°C with 5% CO₂ and 95% humidity.

Cells were seeded in 12-well plates at a density of 1.2×10^5 cells/well and cultured for 3 days. Cell culture medium was replaced with culture medium supplemented with sodium-butyrate (5 mmol/L) 24 hours before transport studies to induce the expression of rOATs and hOATs.

Transport studies

Transport studies were carried out as described previously [15]. The transport activity of rOat1 and rOat3 was assessed using the cells cultured in the dish. The uptake from the basal and apical sides was almost equal when the cells were cultured on porous membrane, suggesting that a similar amount of transporter protein is expressed on the apical and basal membranes of each cDNA-transfected LLC-PK1 cell [15]. Uptake was initiated by adding medium containing radiolabeled compounds after cells had been washed twice and preincubated with Krebs-Henseleit buffer at 37°C for 15 minutes. The Krebs-Henseleit buffer consists of 118 mmol/L NaCl, 4.83 mmol/L KCl, 0.96 mmol/L KH₂PO₄, 1.20 mmol/L MgSO₄, 1.53 mmol/L CaCl₂, 12.5 mmol/L HEPES, 23.8 mmol/L NaHCO₃, 5 mmol/L glucose, and adjusted to pH 7.4. The uptake was terminated at a designated time by adding ice-cold Krebs-Henseleit buffer after removal of the incubation buffer. Then, cells were washed twice with 1 mL ice cold Krebs-Henseleit buffer, dissolved in 500 µL of 0.2 N NaOH, and kept overnight. Aliquots (450 µL) were transferred to scintillation vials after adding 100 µL of 1 N HCl. The radioactivity associated with the cells and medium specimens was determined by liquid scintillation counting after adding scintillation fluid (NACALAI TESQUE, Kyoto, Japan) to the scintillation vials. The remaining 50 µL of the aliquots of cell lysate were used to determine the protein concentration by the method of Lowry with bovine serum albumin as a standard.

Ligand uptake is given as the cell-to-medium concentration ratio determined as the amount of ligand associated with the cells divided by the medium concentration. Specific uptake was obtained by subtracting the uptake into vector-transfected cells from the uptake into cDNA-transfected cells. Kinetic parameters were obtained using the following equation (Michaelis-Menten equation):

One saturable component,

$$v = \frac{V_{\max} \times S}{K_m + S} \quad (1)$$

One saturable (two saturable) and one nonsaturable component,

$$v = \frac{V_{\max 1} \times S}{K_{m1} + S} + \left(\frac{V_{\max 2} \times S}{K_{m2} + S} \right) + CL_{\text{non}} \times S \quad (2)$$

where v is the uptake velocity of the substrate (pmol/min/mg protein), S is the substrate concentration in the medium (µmol/L), K_m is the Michaelis-Menten constant (µmol/L), V_{\max} is the maximum uptake rate (pmol/min/mg protein), and CL_{non} is the nonsaturable uptake clearance. The number of components involved in the uptake by cDNA-transfected cells or kidney slices was determined based on Akaike's Information Criterion (AIC) values [27]. Inhibition constants (K_i values) of a series of compounds were obtained by examining their inhibitory effects on the rOat1/hOAT1- and rOat3/hOAT3-mediated uptake assuming competitive inhibition under the condition that the substrate concentration was much lower than its K_m value using the following equation:

$$CL_{+I} = \frac{CL}{1 + K_i} \quad (3)$$

where CL represents the uptake clearance and the subscript (+I) represents the value in the presence of inhibitor. I represents the concentration of inhibitor (µmol/L). The substrate concentration was low compared with its K_m value in the inhibition study. Fitting was performed by the nonlinear least-squares method using a MULTI program [27] and the Damping Gauss Newton Method algorithm.

Uptake by kidney slices

Uptake studies were carried out as described in a previous report [14]. Slices (0.3 mm thick) of whole kidneys from male Sprague-Dawley rats were put in ice-cold oxygenated incubation buffer. The incubation buffer consisted of 120 mmol/L NaCl, 16.2 mmol/L KCl, 1 mmol/L CaCl₂, 1.2 mmol/L MgSO₄, and 10 mmol/L NaH₂PO₄/Na₂HPO₄ adjusted to pH 7.5. Two slices, each weighing 10 to 20 mg, were randomly selected and then incubated in a 12-well plate with 1 mL oxygenated incubation buffer in each well after slices had been preincubated with incubation buffer for 5 minutes. The uptake study of 1 µmol/L radiolabeled compounds was carried out at 37°C. [¹⁴C]Mannitol (1 µmol/L) was used to estimate the water adhering to the kidney slices in each experiment. After incubating for an appropriate time, each slice was rapidly removed from the incubation buffer, washed in ice-cold saline, blotted on filter paper, weighed, and dissolved in 1 mL of soluene-350 (Perkin Elmer Life Sciences) at 50°C for 3 hours. The radioactivity was determined in a liquid scintillation counter after adding 10 mL of scintillation fluid (Perkin Elmer Life Sciences).

Ligand uptake was given as the amount of ligand associated with the slice specimens divided by the medium concentration. The K_m and K_i values were obtained using equations as described previously.

Estimation of uptake clearance in kidney slices from cDNA-transfected cells

Using the Relative Activity Factor (RAF) concept, we estimated the contribution of rOat1 and rOat3 to the total uptake by kidney slices [16, 28]. A scaling factor for rOat1- and rOat3-mediated transport was obtained using PAH and PCG as reference compounds. The uptake clearances of uremic toxins by cDNA-transfected cells (CL_{rOat1} and CL_{rOat3}) multiplied by R_{rOat1} and R_{rOat3} , respectively, are summarized in Table 3.

$$R_{rOat1} = \frac{CL_{PAH,slice}}{CL_{PAH,rOat1}} \quad (4)$$

$$R_{rOat3} = \frac{CL_{PCG,slice}}{CL_{PCG,rOat3}} \quad (5)$$

$$CL_{test,slice} = CL_{test,rOat1} \cdot R_{rOat1} + CL_{test,rOat3} \cdot R_{rOat3} \quad (6)$$

RESULTS

Uptake of uremic toxins by rOat1- and rOat3-expressing LLC-PK1 cells

The activity of rOat1- and rOat3-expressing LLC-PK1 cells was confirmed in each study by the transport of PAH (1 $\mu\text{mol/L}$) and PCG (1 $\mu\text{mol/L}$), respectively. The mean activities of rOat1- and rOat3-expressing LLC-PK1 cells were 20.1 ± 1.2 and 2.75 ± 0.59 $\mu\text{L}/\text{min}/\text{mg}$ protein, respectively, and these values are comparable to those in a previous report [29].

The time profiles of the uptake of IS, CMPF, IA, and HA by rOat1- and rOat3-expressing, and vector-transfected LLC-PK1 cells are shown in Figure 1. The intracellular accumulation of IS, CMPF, IA, and HA was significantly greater in rOat1-expressing LLC-PK1 cells than in vector-transfected cells. On the other hand, a significant increase in the uptake of IS and CMPF was observed in rOat3-expressing LLC-PK1 cells, but not IA and HA.

The concentration-dependence of the uptake of uremic toxins by rOat1 and rOat3 was investigated (Fig. 2) and kinetic parameters for their uptake are summarized in Table 1. IS had a 10-fold greater K_m value for rOat3 than rOat1. Conversely, CMPF had a 15-fold greater K_m value for rOat1 than rOat3. The transport activities of IS and HA by rOat1 were similar, and these values were approximately 2-fold greater than those of CMPF and IA in rOat1-expressing cells. The transport activity of IS and CMPF by rOat3 was comparable (Table 1).

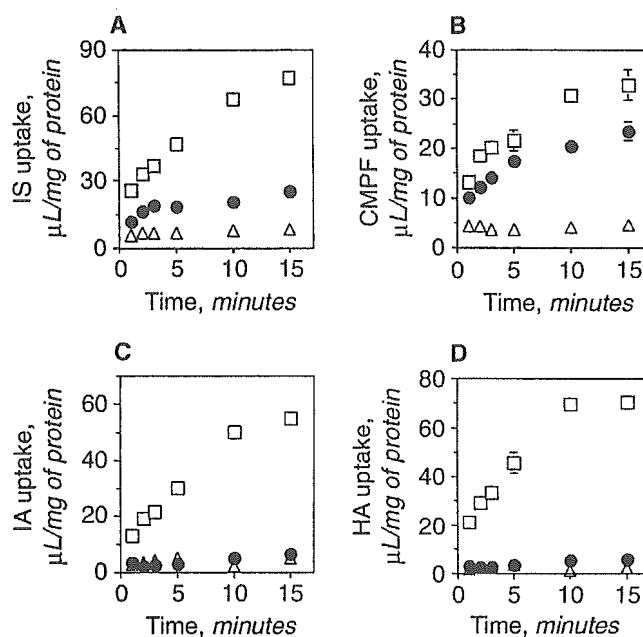


Fig. 1. Time profiles of the uptake of uremic toxins by rat organic anion transporter (rOat)1- and rOat3-expressing pig kidney epithelial cell line (LLC-PK1) cells. (A) The uptake of 1 $\mu\text{mol/L}$ [^3H]IS, (B) 1 $\mu\text{mol/L}$ [^3H]CMPF, (C) 1 $\mu\text{mol/L}$ [^3H]IA, and (D) 1 $\mu\text{mol/L}$ [^{14}C]HA by cDNA-transfected cells was examined at 37°C. Squares, closed circles, and triangles represent the uptake by rOat1- and rOat3-expressing cells and vector-transfected LLC-PK1 cells, respectively. Each point represents the mean \pm SE ($N = 3$). Abbreviations are: IS, indoxyl sulfate; CMPF, 3-carboxy-4-methyl-5-propyl-2-furanpropionate; IA, indoleacetate; HA, hippurate.

The inhibitory effect of uremic toxins on the uptake via rOat1 and rOat3 is shown in Figure 3. The K_i values obtained assuming competitive inhibition are summarized in Table 2. The K_i value of IS for rOat1 was smaller than that for rOat3, and the K_i value of CMPF for rOat3 was smaller than that for rOat1. These results agreed with the results obtained by the Eadie-Hofstee plots as shown in Table 1. The K_i values of IA and HA were determined for the uptake of PCG by rOat3, because no significant uptake of IA and HA was observed in rOat3-transfected cells. HA inhibited the transport by rOat3 with a K_i value similar to the K_m and K_i values for rOat1. IA inhibited the transport via rOat3, but the K_i value for rOat3 was much greater than that for rOat1.

Uptake of uremic toxins by kidney slices

The activity of kidney slices was confirmed in each study by the uptake of PAH (1 $\mu\text{mol/L}$) and PCG (1 $\mu\text{mol/L}$). The mean uptake clearance of PAH and PCG was 0.276 ± 0.018 and 0.200 ± 0.004 $\text{mL}/\text{min}/\text{g}$ of kidney, respectively.

The time profiles and the concentration-dependence of the uptake of uremic toxins by rat kidney slices are shown in Figure 4. The K_m and V_{max} values obtained by kinetic analysis are summarized in Table 1. Analysis of the

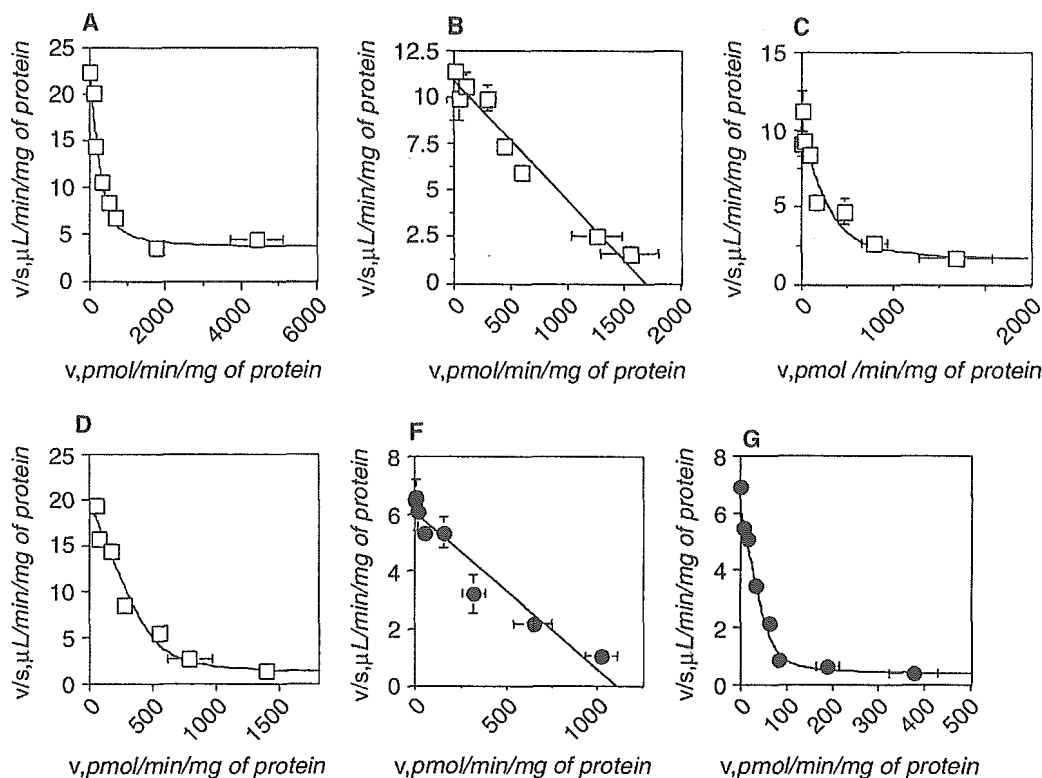


Fig. 2. Eadie-Hofstee plots of the uptake of uremic toxins by rat organic anion transporter (rOat)1- and rOat3-expressing pig kidney epithelial cell line (LLC-PK1) cells. (A and E) The concentration dependence of [^3H]IS, (B and F) [^3H]CMPF, (C) [^3H]IA, and (D) [^{14}C]HA by cDNA-transfected cells is shown. Squares and closed circles represent the uptake by rOat1- and rOat3-expressing cells, respectively. The uptake by rOat1- and rOat3-expressing cells was measured for 1 minute and 2 minutes at various concentrations (IS, CMPF, and IA, 0.3–1000 $\mu\text{mol/L}$; HA, 2–1000 $\mu\text{mol/L}$). The rOat1- and rOat3-mediated transports were obtained by subtracting the transport velocity in vector-transfected cells from those in rOat1- and rOat3-expressing cells. Each point represents the mean \pm SE ($N = 3$). Abbreviations are: IS, indoxyl sulfate; CMPF, 3-carboxy-4-methyl-5-propyl-2-furanpropionate; IA, indoleacetate; HA, hippurate.

Table 1. Kinetic parameters of the uptake of uremic toxins PAH and PCG by rOat1-, rOat3-expressing LLC-PK1 cells, and kidney slices

	rOat1-LLC-PK1			rOat3-LLC-PK1			Kidney slice		
	K_m $\mu\text{mol/L}$	V_{max} pmol/min/mg of protein	V_{max}/K_m $\mu\text{L/min/mg}$ of protein	K_m $\mu\text{mol/L}$	V_{max} pmol/min/mg of protein	V_{max}/K_m $\mu\text{L/min/mg}$ of protein	K_m $\mu\text{mol/L}$	V_{max} nmol/min/g of kidney	V_{max}/K_m mL/min/g of kidney
IS	17.7 ± 5.3	350 ± 80	19.7 (3.42 ± 0.39)	174 ± 24	1047 ± 115	6.02	24.1 ± 11.1 19.6 ± 44	1.48 ± 1.16 19.6 ± 1.2	0.061 0.100 (0.039 ± 0.001)
CMPF	154 ± 14	1669 ± 114	10.8	10.9 ± 2.0	66.4 ± 9.2	6.09 (0.33 ± 0.04)	22.4 ± 7.0	5.40 ± 1.45	0.241 (0.068 ± 0.007)
IA	47.1 ± 17.3	387 ± 131	8.22 (1.39 ± 0.30)	–	–	–	41.5 ± 6.5	8.08 ± 1.18	0.195 (0.076 ± 0.004)
HA	27.5 ± 4.7	519 ± 69	18.9 (0.92 ± 0.15)	–	–	–	33.0 ± 3.2	8.96 ± 0.67	0.272 (0.015 ± 0.001)
PAH	–	–	20.1	–	–	–	–	–	0.276
PCG	–	–	–	–	–	2.75	–	–	0.200

Abbreviations are: rOat, rat organic anion transporter; LLC-PK1, pig kidney epithelial cell line; PAH, *p*-aminohippurate; PCG, benzyl-penicillin; IS, indoxyl sulfate; IA, indoleacetate; HA, hippurate; CMPF, 3-carboxy-4-methyl-5-propyl-2-furanpropionate.

Data shown in Figures 2 and 4 were used to determine the kinetic parameters for the uptake of organic anions by cDNA-transfected cells and kidney slices. CL_{non} values are given in parentheses. These parameters were determined by nonlinear regression analysis. Reproducibility of the transport activities by cDNA-transfected cells and kidney slices (V_{max}/K_m) was confirmed by 4–10 individual experiments. In every experiment, PAH and PCG were used as reference compounds to check the transport activity by cDNA-transfected cells and kidney slices. Each value represents the mean \pm SD ($N = 3$).

uptake of IS by kidney slices revealed two saturable and one nonsaturable components (K_{m1} and $V_{max1} = 24.1 \pm 11.2 \mu\text{mol/L}$ and $1.48 \pm 1.16 \text{ nmol/min/g}$ of kidney; K_{m2} and $V_{max2} = 196 \pm 44 \mu\text{mol/L}$ and $19.6 \pm 1.2 \text{ nmol/min/g}$

of kidney; $CL_{non} = 0.039 \pm 0.001 \text{ mL/min/g}$ of kidney), although only one saturable and one nonsaturable component were observed in the uptake of CMPF, IA, and HA (Fig. 4).

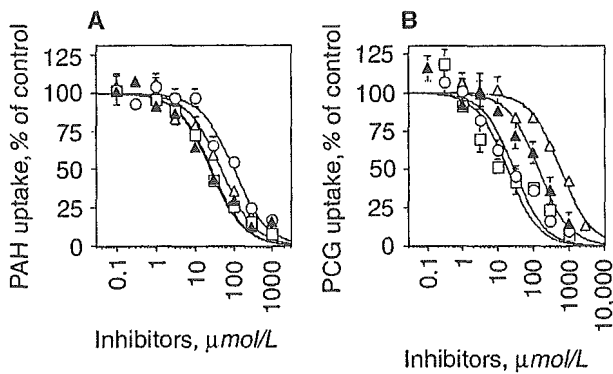


Fig. 3. Inhibitory effect of uremic toxins on the uptake of [³H]PAH and [³H]PCG by rat organic anion transporter (rOat1)- and rOat3-expressing pig kidney epithelial cell line (LLC-PK1) cells. rOat1-mediated 1 μmol/L [³H]PAH uptake for 1 minute and rOat3-mediated 1 μmol/L [³H]PCG uptake for 2 minutes were determined in the presence and absence of unlabeled IS (▲), CMPF (○), IA (△), and HA (□) at the designated concentrations. The values are expressed as a percentage of the uptake in the absence of any unlabeled compounds. Solid lines represent the fitted line obtained by nonlinear regression analysis. Each point represents the mean ± SE (N = 3). Abbreviations are: IS, indoxyl sulfate; CMPF, 3-carboxy-4-methyl-5-propyl-2-furanpropionate; IA, indoleacetate; HA, hippurate; PAH, *p*-aminohippurate; PCG, benzylpenicillin.

Table 2. *K_i* values of uremic toxins uptake by rOat1- and rOat3-expressing LLC-PK1 cells

Inhibitor	PAH uptake <i>K_i</i> for rOat1-LLC-PK1	PCG uptake <i>K_i</i> for rOat3-LLC-PK1
IS	25.0 ± 6.4	138 ± 38
CMPF	103 ± 21	27.9 ± 9.3
IA	48.5 ± 10.8	582 ± 113
HA	27.5 ± 4.3	18.6 ± 10.7

For abbreviations, see Table 1. The *K_i* values were determined by nonlinear regression analysis. Data are taken from Figure 3. Units of *K_i* values are μmol/L. Each value represents the mean ± SD (N = 3).

Estimation of uptake clearance in kidney slices from cDNA-transfected cells

The contributions of rOat1 and rOat3 to the renal uptake of IS and CMPF were estimated based on the RAF concept [16, 28]. The transport activities of IS and CMPF by rOat1 and rOat3 were corrected by scaling factors for rOat1 and rOat3 (*R_{rOat1}* and *R_{rOat3}*, respectively). Comparison of the corrected transport activity by rOat1 and rOat3 suggested that the contribution of rOat1 and rOat3 to the uptake of IS was 38% and 62%, respectively, and that the corresponding values for CMPF uptake were 25% and 75%, respectively (Table 3).

The uptake clearances of uremic toxins by kidney slices were predicted using the transport activities by cDNA-transfected cells and scaling factors for rOat1 and rOat3 (Table 3). The absolute values for IA and HA uptake were comparable between the predicted and observed values, whereas the predicted values of IS and CMPF were greater than the observed values (Table 3).

Effect of inhibitors on the uptake of uremic toxins by rOat1-, rOat3-expressing LLC-PK1 cells, and kidney slices

Figure 5 shows the inhibitory effect of PAH and PCG on the uptake of uremic toxins by rOat1- and rOat3-expressing LLC-PK1 cells. The *K_i* values of PAH for rOat1- and rOat3-mediated transport were found to be about 50 μmol/L and 1 mmol/L, respectively (Table 4). The *K_i* values of PCG for rOat1- and rOat3-mediated transport were about 2 mmol/L and 100 μmol/L, respectively. These values agreed with previous reports [14, 29], suggesting that PAH and PCG are selective inhibitors of rOat1 and rOat3. However, PCG inhibited the uptake of IA by rOat1 at a smaller *K_i* value compared with those for the uptake of other uremic toxins by rOat1. The contribution of rOat1 and rOat3 will be evaluated by examining their inhibitory effect of the uptake of uremic toxins by kidney slices. The inhibitory effects of these inhibitors on the uptake of uremic toxins by kidney slices were examined (Fig. 6), and their *K_i* values were summarized in Table 4. DBSP, a nonspecific inhibitor for organic anion transporters, markedly inhibited the uptake of uremic toxins by kidney slices with *K_i* values similar to those for PAH and pravastatin uptake by kidney slices (Fig. 6) [14]. The degree of inhibition by 300 μmol/L PAH, 100 μmol/L pravastatin, and 300 μmol/L PCG, which selectively inhibit either rOat1 or rOat3, on the uptake of IS was approximately 45%, 60%, and 65%, respectively. The corresponding values were found to be approximately 30%, 70%, and 75%, respectively, for the uptake of CMPF, and 70%, 5%, and 10%, respectively, for the uptake of HA. The inhibitory effect of 300 μmol/L PAH on the uptake of IA was about 80%.

Uptake of uremic toxins by hOAT1- and hOAT3-expressing HEK293 cells

The time profiles of the uptake of IS, CMPF, IA, and HA by hOAT1- and hOAT3-expressing and vector-transfected HEK293 cells are shown in Figure 7. The intracellular accumulation of IS, CMPF, IA, and HA was significantly greater in hOAT1-expressing cells than in vector-transfected cells. On the other hand, a significant increase in the uptake of IS and CMPF was observed in hOAT3-expressing HEK293 cells, but not in the case of IA and HA. The *K_m* and *V_{max}* values were determined by kinetic analysis (Fig. 8). As shown in Table 5, the kinetic parameters for hOATs-expressing transfectants were very similar to those obtained for rOats-expressing cells (Table 1). The inhibitory effect of uremic toxins on the uptake via hOAT1 and hOAT3 is shown in Figure 9. The *K_i* values obtained assuming competitive inhibition are summarized in Table 6. These values also agreed with those obtained for rOats-expressing cells as shown in Table 2.

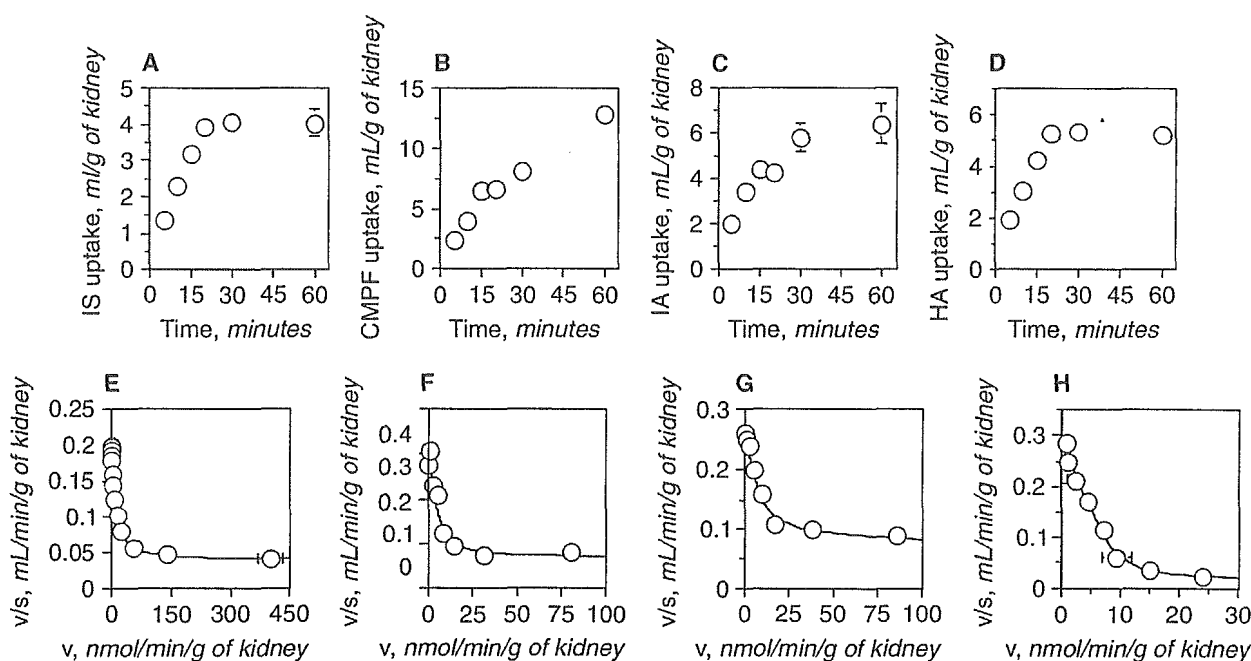


Fig. 4. Time profiles and Eadie-Hofstee plots of the uptake of uremic toxins by kidney slices. The uptake of (A) 1 $\mu\text{mol/L}$ [^3H]IS, (B) 1 $\mu\text{mol/L}$ [^3H]CMPF, (C) 1 $\mu\text{mol/L}$ [^3H]IA, and (D) 1 $\mu\text{mol/L}$ [^{14}C]HA by kidney slices was examined at 37°C. The concentration dependence of (E) [^3H]IS, (F) [^3H]CMPF, (G) [^3H]IA, and (H) [^{14}C]HA are shown as Eadie-Hofstee plots. The uptake by kidney slices was measured at concentrations between 1 $\mu\text{mol/L}$ and 10 mmol/L IS, and between 1 $\mu\text{mol/L}$ and 1 mmol/L other toxins for 15 minutes at 37°C. Adherent water was determined by the uptake of mannitol, and that was subtracted from the distribution volume of uremic toxins. Each point represents the mean \pm SE ($N = 3$). Abbreviations are: IS, indoxyl sulfate; CMPF, 3-carboxy-4-methyl-5-propyl-2-furanpropionate; IA, indoleacetate; HA, hippurate.

Table 3. Comparison of uptake clearance in kidney slices with predicted values from the uptake study using rOat1- and rOat3-expressing LLC-PK1 cells

	rOat1-mediated uptake	rOat3-mediated uptake	Predicted value	Observed value
	<i>mL/min/g of kidney</i>			
IS	0.271 (38%)	0.438 (62%)	0.709	0.161
CMPF	0.149 (25%)	0.443 (75%)	0.592	0.241
IA	0.113	—	0.113	0.195
HA	0.260	—	0.260	0.272

For abbreviations, see Table 1. The intrinsic transport activities of uremic toxins in cDNA-transfected cells (V_{max}/K_m) were obtained from Table 1. The observed values represent the intrinsic transport activity by kidney slices. The intrinsic clearance of the component whose K_m value is comparable with that of the uptake in cDNA-transfected cells was used for the uptake of IS and CMPF. The contribution of rOat1- and rOat3-mediated transport was given in parentheses. The R_{rOat1} and R_{rOat3} were 13.8×10^{-3} and 72.7×10^{-3} , respectively. The details of the calculation were described in Methods.

DISCUSSION

In the present study, we investigated the renal uptake mechanism of uremic toxins, focusing on the contribution of rOat1 and rOat3. The contribution of each transporter was evaluated by saturation kinetics, RAF analysis, and by examining the effect of inhibitors relatively selective for rOat1 and rOat3.

rOat1-expressing LLC-PK1 cells exhibited marked accumulation of IS, CMPF, IA, and HA, while rOat3-expressing LLC-PK1 cells exhibited significant uptake of only IS and CMPF. IS had a 10-fold greater K_m value for rOat3 than rOat1, and the transport activity of IS was greater in rOat1-expressing cells than in rOat3-expressing cells. Conversely, CMPF had a 15-fold greater K_m value for rOat1 than rOat3, but the transport activ-

ities of rOat1 and rOat3 were similar (Fig. 2, Table 1). Kinetic analysis of IS uptake by kidney slices revealed two saturable and one nonsaturable components (Fig. 4), and the K_m values of IS for the high- and low-affinity components were comparable with those of rOat1 and rOat3, respectively. In the uptake of other uremic toxins by kidney slices, one saturable and one nonsaturable component was observed. The K_m value of CMPF for the uptake by kidney slices was comparable with that of rOat3, while the K_m values of IA and HA for the uptake by kidney slices agreed with those of rOat1. These results suggest that both rOat1 and rOat3 are involved in the renal uptake of IS as high- and low-affinity sites, and rOat1 and rOat3 are involved in the renal uptake of IA and HA, and CMPF, respectively.

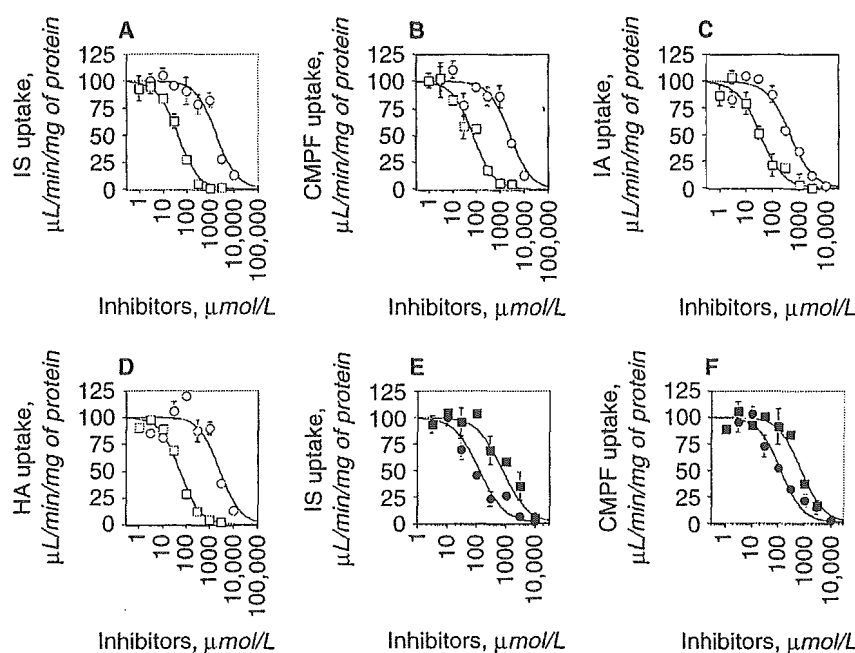


Fig. 5. Inhibitory effect of PAH and PCG on the uptake of uremic toxins by rOat1- and rOat3-expressing LLC-PK1 cells. rOat1-mediated (A) 1 $\mu\text{mol/L}$ [^3H]IS, (B) 1 $\mu\text{mol/L}$ [^3H]CMPF, (C) 1 $\mu\text{mol/L}$ [^3H]IA, and (D) 2 $\mu\text{mol/L}$ [^{14}C]HA uptake for 1 minute were determined in the presence and absence of unlabeled PAH (\square) and PCG (\circ) at the designated concentrations. (E) rOat3-mediated 1 $\mu\text{mol/L}$ [^3H]IS and (F) 1 $\mu\text{mol/L}$ [^3H]CMPF uptake for 2 minutes were determined in the presence and absence of unlabeled PAH (\blacksquare) and PCG (\bullet). The values are expressed as a percentage of the uptake in the absence of any unlabeled compounds. Solid lines represent the fitted line obtained by nonlinear regression analysis. Each point represents the mean \pm SE ($N = 3$). Abbreviations are: rOat, rat organic anion transporter; LLC-PK1, pig kidney epithelial cell line; IS, indoxyl sulfate; CMPF, 3-carboxy-4-methyl-5-propyl-2-furanpropionate; IA, indoleacetate; HA, hippurate; PAH, *p*-aminohippurate; PCG, benzylpenicillin.

The contribution of rOat1 and rOat3 was quantified in stable transformants by comparing their transport activities corrected by the corresponding RAF values (Table 3). The predicted contribution of rOat1 and rOat3 to the uptake of IS by kidney slices was approximately 40% and 60%, respectively. These values were comparable with those of the high- and low-affinity component for IS uptake by kidney slices. The corresponding values for CMPF were approximately 25% and 75%, respectively (Table 3). This was consistent with the observation that the saturable component accounting for the majority of CMPF uptake by kidney slices showed a K_m value comparable with that for rOat3. The predicted and observed uptake clearance of IA and HA were in good agreement, whereas the predicted clearances of IS and CMPF were several-fold greater than the observed values in kidney slices (Table 3). The RAF method may not be applicable to all substrates, and further studies are needed to describe the limitations of the RAF method in predicting *in vivo* clearance from cDNA-transfected cells.

Furthermore, the contribution of rOat1 and rOat3 to the total renal uptake of uremic toxins by kidney slices was evaluated by examining the effect of relatively selective inhibitors of rOat1 and rOat3 (Fig. 6). PAH, pravastatin, and PCG have been shown to exhibit a great difference in their K_m or K_i values for rOat1 and rOat3 [14, 29]. In a recent study, the K_i value of PAH for the uptake by rOat3 was calculated to be about 1 mmol/L, which was 20-fold greater than the K_i value for the rOat1-mediated uptake ($K_i =$ about 50 $\mu\text{mol/L}$). PCG exhibited a much higher affinity for rOat3 ($K_m =$ about 100 $\mu\text{mol/L}$) than for rOat1 ($K_i =$ about 2 mmol/L) (Fig. 5, Table 4). These observations agree with previous reports [14, 29]. In addition, pravastatin has been reported to exhibit a much higher affinity for rOat3 ($K_m =$ 13 $\mu\text{mol/L}$)

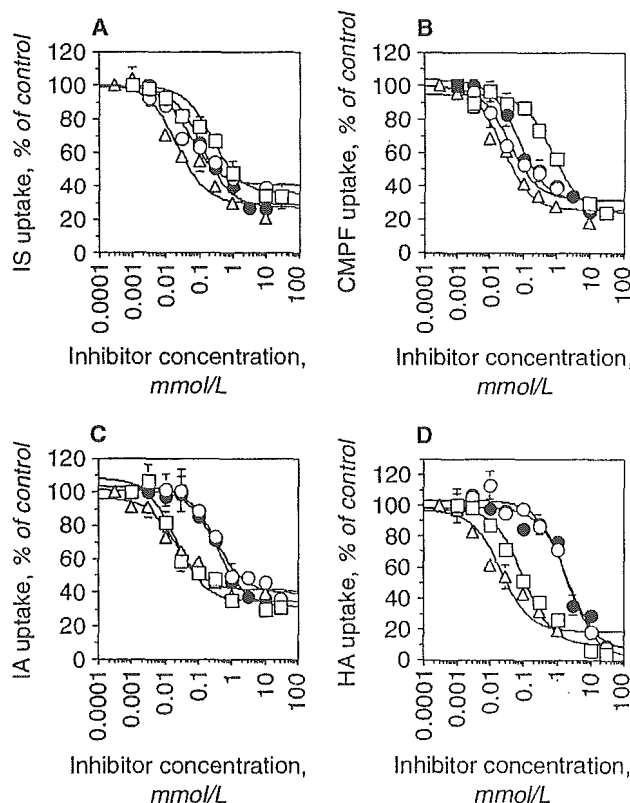


Fig. 6. Inhibitory effect of PAH, pravastatin, and DBSP on the uptake of uremic toxins by kidney slices. The uptake of (A) 1 $\mu\text{mol/L}$ [^3H]IS, (B) 1 $\mu\text{mol/L}$ [^3H]CMPF, (C) 1 $\mu\text{mol/L}$ [^3H]IA, and (D) 1 $\mu\text{mol/L}$ [^{14}C]HA for 15 minutes by kidney slices was determined in the presence and absence of unlabeled PAH (\square), pravastatin (\circ), PCG (\bullet), and DBSP (Δ) at the designated concentrations. The values are expressed as a percentage of the uptake in the absence of any unlabeled compounds. Solid lines represent the fitted line obtained by nonlinear regression analysis. Each point represents the mean \pm SE ($N = 3$). Abbreviations are: IS, indoxyl sulfate; CMPF, 3-carboxy-4-methyl-5-propyl-2-furanpropionate; IA, indoleacetate; HA, hippurate; PAH, *p*-aminohippurate; PCG, benzylpenicillin; DBSP, dibromosulfophthalein.

Table 4. K_i values for the uptake of uremic toxins by rOat1-, rOat3-expressing LLC-PK1 cells, and kidney slices

Inhibitor	IS uptake			CMPF uptake			IA uptake		HA uptake	
	rOat1-LLC-PK1	rOat3-LLC-PK1	Kidney slice	rOat1-LLC-PK1	rOat3-LLC-PK1	Kidney slice	rOat1-LLC-PK1	Kidney slice	rOat1-LLC-PK1	Kidney slice
PAH	42.4 ± 6.7	1283 ± 333	-	75.2 ± 21.5	808 ± 204	781 ± 154	35.6 ± 9.5	20.5 ± 7.6	54.0 ± 9.9	100 ± 27
PCG	1890 ± 547	96.8 ± 30.9	-	2763 ± 978	132 ± 38	73.4 ± 21.1	470 ± 134	354 ± 46	2785 ± 1386	2082 ± 698
Pravastatin	-	-	-	-	-	37.9 ± 13.8	-	315 ± 76	-	1966 ± 537
DBSP	-	-	21.6 ± 9.4	-	-	23.9 ± 6.7	-	20.4 ± 6.8	-	21.7 ± 10.1

For abbreviations, See Table 1. The effects of PAH, PCG, pravastatin, and DBSP were examined on the uptake of uremic toxins by cDNA-transfected cells and kidney slices. The K_i values were determined by nonlinear regression analysis. Reliable K_i values of the inhibitors for the uptake of IS by kidney slices were not obtained. Data are taken from Figures 5 and 6. Units of K_i values are $\mu\text{mol/L}$. Each value represents the mean \pm SD ($N = 3$).

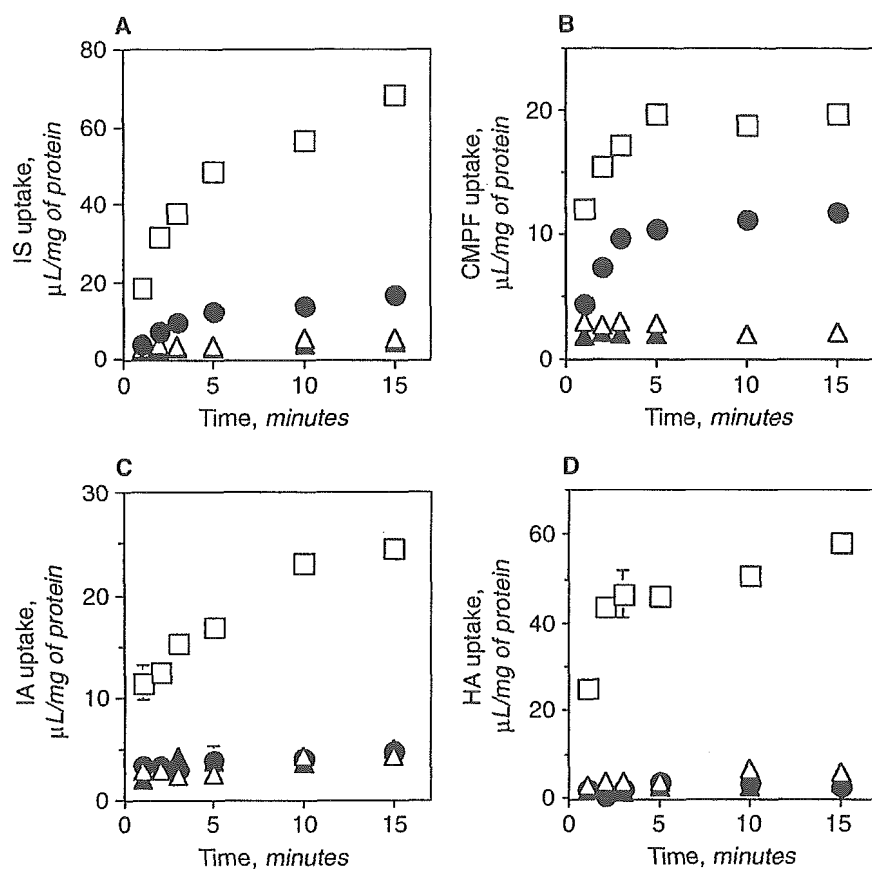


Fig. 7. Time profiles of the uptake of uremic toxins by hOAT1- and hOAT3-expressing HEK293 cells. The uptake of (A) 1 $\mu\text{mol/L}$ [^3H]IS, (B) 1 $\mu\text{mol/L}$ [^3H]CMPF, (C) 1 $\mu\text{mol/L}$ [^3H]IA, and (D) 1 $\mu\text{mol/L}$ [^{14}C]HA by cDNA-transfected cells was examined at 37°C. Squares, closed circles, and triangles (Δ), vector for hOAT1; \blacktriangle , vector for hOAT3 represents the uptake by hOAT1- and hOAT3-expressing cells and vector-transfected HEK293 cells, respectively. Each point represents the mean \pm SE ($N = 3$). Abbreviations are: IS, indoxyl sulfate; CMPF, 3-carboxy-4-methyl-5-propyl-2-furanpropionate; IA, indoleacetate; HA, hippurate; hOAT, human organic anion transporter.

than for rOat1 ($K_i = 1.2 \text{ mmol/L}$) [14]. Taking into consideration the kinetic parameters of these inhibitors, 300 $\mu\text{mol/L}$ PAH will saturate rOat1-mediated transport, but will have only a minimal effect on the rOat3-mediated uptake at this concentration. Therefore, the degree of inhibition for saturable uptake by kidney slices by PAH at 300 $\mu\text{mol/L}$ represents the contribution of rOat1 to the renal uptake of uremic toxins (IS, 45%; CMPF, 30%; IA, 80%; HA, 70% inhibition of the total saturable component). Moreover, the K_i values of PAH for the uptake of IA and HA by kidney slices were comparable with those for rOat1 (Table 4). As for rOat3, the inhibitory effects of 100 $\mu\text{mol/L}$ pravastatin (IS, 60%; CMPF, 70%; HA, 5% inhibition of the total saturable component) and

300 $\mu\text{mol/L}$ PCG (IS, 65%; CMPF, 75%; HA, 10% inhibition of the total saturable component) represents its contribution. Inhibitory effect of PAH and PCG showed different potency for the uptake of IA and HA by rOat1-expressing cells. Their K_i values for IA uptake by rOat1 were 5- and 6-fold smaller than those for HA (Table 4). This effect was also observed in kidney slices, in which the K_i values of PAH and PCG for the uptake of IA were smaller than those for HA, but comparable with those for rOat1-mediated uptake of IA. A similar phenomenon was also observed in the inhibitory effect of pravastatin, whose K_i value for the uptake of IA by kidney slices was markedly smaller than that of HA (Table 4). The contribution of rOat1 and rOat3 to the renal uptake of uremic

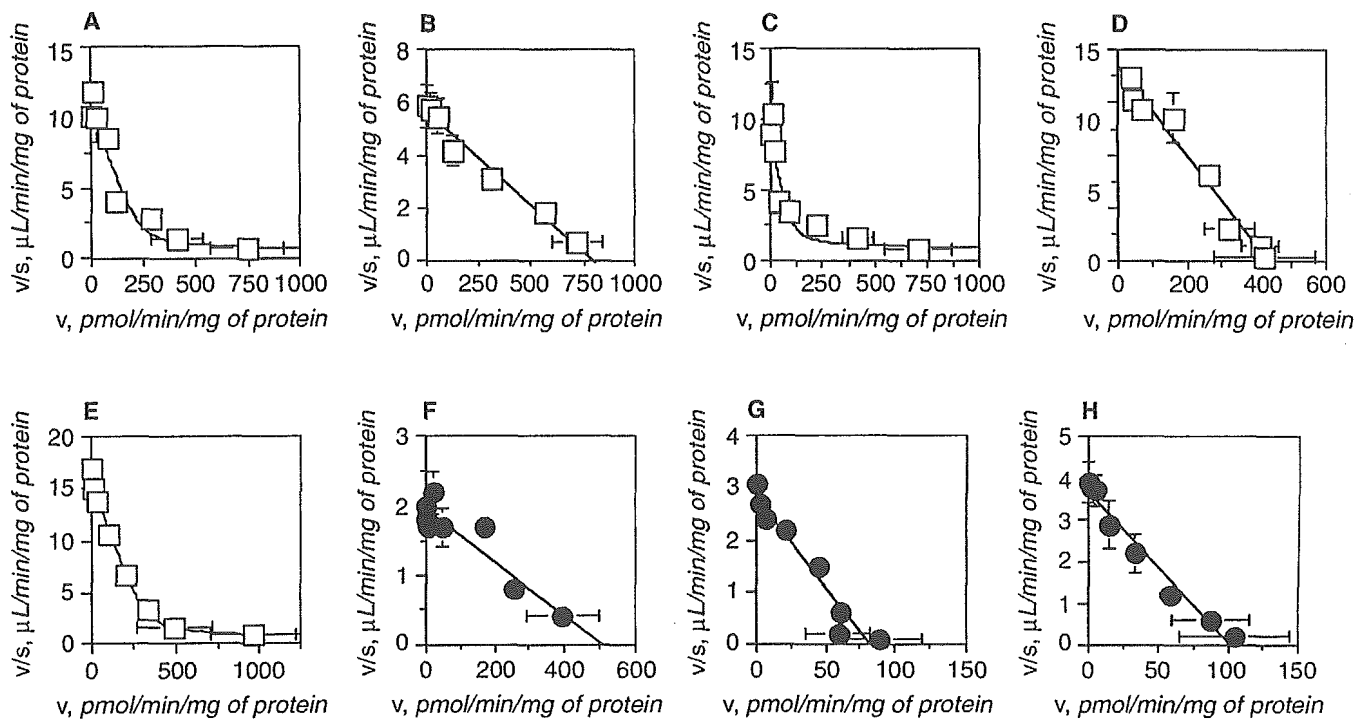


Fig. 8. Eadie-Hofstee plots of the uptake of uremic toxins PAH and PCG by hOAT1- and hOAT3-expressing HEK293 cells. The concentration dependence of (A and F) [³H]IS, (B and G) [³H]CMPF, (C) [³H]IA, (D) [¹⁴C]HA, (E) [³H]PAH, and (H) [³H]PCG by cDNA-transfected cells is shown. The uptake by hOAT1-expressing cells (A-E) was measured for 1 minute (uremic toxins) and 2 minutes (PAH) at various concentrations (IS, CMPF, IA, and PAH, 0.3–1000 μmol/L, HA, 2–1000 μmol/L). The uptake by hOAT3-expressing cells (F-H) was measured for 3 minutes at various concentrations (0.3–1000 μmol/L). The hOAT1- and hOAT3-mediated transports were obtained by subtracting the transport velocity in vector-transfected cells from those in hOAT1- and hOAT3-expressing cells. Each point represents the mean ± SE (N = 3). Abbreviations are: IS, indoxyl sulfate; CMPF, 3-carboxy-2-methyl-5-propyl-2-furanpropionate; IA, indoleacetate; HA, hippurate; PAH, *p*-aminohippurate; PCG, benzylpenicillin; hOAT, human organic anion transporter

Table 5. Kinetic parameters of the uptake of uremic toxins PAH and PCG by hOAT1- and hOAT3-expressing HEK293 cells

	hOAT1-HEK293			hOAT3-HEK293		
	K_m μmol/L	V_{max} pmol/min/mg of protein	V_{max}/K_m μL/min/mg of protein	K_m μmol/L	V_{max} pmol/min/mg of protein	V_{max}/K_m μL/min/mg of protein
IS	20.5 ± 5.3	216 ± 45	10.5 (0.573 ± 0.127)	263 ± 40	505 ± 63	1.92
CMPF	141 ± 10	801 ± 45	5.67	26.5 ± 3.0	76.5 ± 5.7	2.89
IA	14.0 ± 8.1	110 ± 50	7.86 (0.897 ± 0.224)	-	-	-
HA	23.5 ± 1.7	430 ± 19	18.3	-	-	-
PAH	20.1 ± 1.4	308 ± 18	15.4 (0.670 ± 0.048)	-	-	-
PCG	-	-	-	54.0 ± 4.9	198 ± 13	3.67

For abbreviations, see Table 1. Data shown in Figure 8 were used to determine the kinetic parameters for the uptake of uremic toxins by cDNA-transfected cells. CL_{non} values are given in parentheses. These parameters were determined by nonlinear regression analysis. Reproducibility of the transport activities by cDNA-transfected cells (V_{max}/K_m) was confirmed by 3-7 individual experiments. In every experiment, PAH and PCG were used as reference compounds to check the transport activity by cDNA-transfected cells and kidney slices. Each value represents the mean ± SD (N = 3).

toxins determined by the three different methods was in a good agreement; rOat1 and rOat3 equally contribute to the renal uptake of IS. rOat1 mainly accounts for IA and HA uptake, whereas rOat3 accounts for CMPF uptake. Previously, in an in vivo study using the KUI technique, it was proposed that rOat3 mainly contributes to the renal uptake of IS, in which the renal uptake of IS was significantly inhibited by PAH and PCG [22]. Taking the present

results into consideration, inhibition by PAH and PCG in an in vivo study supports the involvement of both rOat1 and rOat3 in the renal uptake of IS. In the previous study, lack of inhibition by indomethacin was interpreted as a minor contribution of rOat1 [22]. However, because indomethacin is highly associated with plasma protein, its insufficient blood concentration after intra-arterial injection may account for this discrepancy.

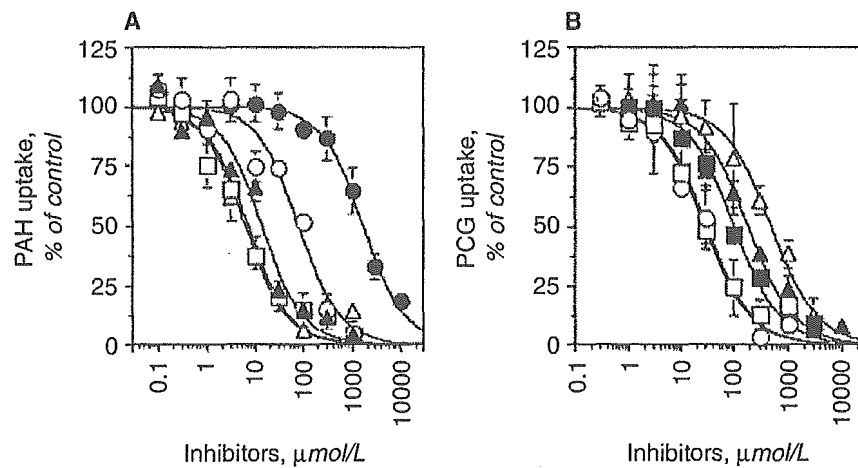


Fig. 9. Inhibitory effect of uremic toxins on the uptake of [³H]PAH and [³H]PCG by hOAT1- and hOAT3-expressing HEK293 cells. The uptake of (A) [³H]PAH and (B) [³H]PCG by hOAT1 and hOAT3 was determined in the presence and absence of unlabeled IS (Δ), CMPF (\circ), IA (\triangle), HA (\square), PAH (\blacksquare), and PCG (\bullet) at the designated concentrations. The values are expressed as a percentage of the uptake in the absence of any unlabeled compounds. Solid lines represent the fitted line obtained by nonlinear regression analysis. Each point represents the mean \pm SE ($N = 3$). Abbreviations are: IS, indoxyl sulfate; CMPF, 3-carboxy-4-methyl-5-propyl-2-furanpropionate; IA, indoleacetate; HA, hippurate; PAH, *p*-aminohippurate; PCG, benzylpenicillin; hOAT, human organic anion transporter.

Table 6. K_i values of uremic toxins PAH and PCG uptake by hOAT1- and hOAT3-expressing HEK293 cells

Inhibitor	K_i for hOAT1 $\mu\text{mol/L}$	K_i for hOAT3 $\mu\text{mol/L}$	Healthy volunteers ^a		Predialysis patients ^a	
			Total concentration $\mu\text{mol/L}$	Unbound concentration $\mu\text{mol/L}$	Total concentration $\mu\text{mol/L}$	Unbound concentration $\mu\text{mol/L}$
IS	13.2 \pm 3.3	183 \pm 44	4.10	0.16	104	12.9
CMPF	247 \pm 63	27.9 \pm 5.1	15.1	0.15 ^b	183	1.83 ^b
IA	21.0 \pm 6.0	491 \pm 57	1.45	0.44	26.3	3.92
HA	18.8 \pm 4.7	30.8 \pm 6.5	13.3	3.99 ^b	271	122
PAH	-	100 \pm 13	-	-	-	-
PCG	1703 \pm 151	-	-	-	-	-

For abbreviations, see Table 1. The K_i values were determined by nonlinear regression analysis. Data are taken from Figure 9. Each value represents the mean \pm SD ($N = 3$)

^a Sakai et al (1996)

^b The unbound plasma concentrations were calculated from the total plasma concentrations and unbound fractions of CMPF (1%) and HA (30%), Niwa et al, 1996

The contribution of rOat3 to the uptake of IS and CMPF by kidney slices was comparable to or greater than that of rOat1, even though the transport activities of IS and CMPF by rOat1 were greater or comparable with those by rOat3. Taking into consideration the relatively large difference in the scaling factors for rOat1 and rOat3, this may be accounted for by the difference in their protein expression in the kidney, and/or the maintenance of their driving force in the host cells. Further studies, especially quantification of the protein expression of rOat1 and rOat3 in the kidney, are needed to overcome this discrepancy.

The human isoforms of rOat1 and rOat3, hOAT1 and hOAT3, are predominantly expressed in the kidney and localized on the basolateral membrane of the proximal tubules [17–19]. hOAT1 exhibited significant uptake of IS, CMPF, IA, and HA, while hOAT3 exhibited uptake of IS and CMPF (Fig. 7). Furthermore, the K_m and K_i values for the uptake of uremic toxins by hOAT1 and hOAT3 were almost comparable with those for the uptake by rOat1 and rOat3. Thus, there was a minimal species difference, at least in the K_m values of uremic toxins, between rats and humans. Using PAH as a reference substrate, the relative transport activities of hOAT1 for the uptake of uremic toxins (IS, 0.68; CMPF, 0.37;

IA, 0.51; HA, 1.19) were very similar to those of rOat1 (IS, 0.98; CMPF, 0.54; IA, 0.41; HA, 0.94) (Tables 1 and 5). However, the relative transport activities of IS and CMPF were lower in hOAT3 (IS, 0.52; CMPF, 0.79) than in rOat3 (IS, 2.19; CMPF, 2.21). The unbound concentration of uremic toxins in normal serum is lower than the K_m values for hOAT1 and hOAT3 (IS, 0.16 $\mu\text{mol/L}$; CMPF, 0.15 $\mu\text{mol/L}$; IA, 0.44 $\mu\text{mol/L}$; HA, 3.99 $\mu\text{mol/L}$) [4, 30], and thus, the uptake by OATs should occur under linear conditions. Assuming that the scaling parameters are similar in rat and human, it is possible that the contribution of hOAT3 to the renal uptake of IS and CMPF in humans is smaller than in rat. This should be examined in future studies, possibly using freshly prepared human kidney slices.

Residual nephrons make a significant contribution to the removal of uremic waste products in patients on chronic dialysis treatment [31]. IS, CMPF, IA, and HA accumulate in uremic serum up to levels of 417, 370, 101, and 883 $\mu\text{mol/L}$, respectively [30, 32], and these compounds depresses PAH transport by the kidney [20, 21]. The present study proposes that hOAT1 and hOAT3 are potential sites of interaction between uremic toxins and endogenous or exogenous compounds. The unbound serum concentrations of uremic toxins are listed in Table 6 [4,

30], and the unbound serum concentrations of IS and HA in predialysis patients were comparable with the K_m and K_i values for hOAT1 and hOAT3. Therefore, it is possible that IS and HA inhibit hOAT1- or hOAT3-mediated transport in vivo in predialysis patients, leading to acceleration of serum accumulation of uremic toxins, and reduction of the plasma elimination of drugs via hOAT1 and hOAT3.

It has been demonstrated that active tubular secretion is involved in the urinary excretion of IS, CMPF, IA, and HA in rats, because their renal clearances were greater than the glomerular filtration rate [2]. Also, the renal clearance of IS and HA has been reported to be 29 and 590 mL/min in healthy people [33, 34]. Considering the serum protein binding of IS (90–96%) and HA (70%) [4, 30], renal elimination of IS and HA into urine is mediated by tubular secretion. To achieve the vectorial transport of organic anions, it is likely that transporter(s) are involved in the secretion across the brush border membrane of the proximal tubules. It has been demonstrated that the renal brush border membrane possesses an influx/efflux transport system for organic anions, such as organic anion transporting polypeptide 1 (Oatp1; *Slc21a1*), Oat-K1 (*Slc21a4*), Oat-K2, multidrug resistance associated protein 2 (Mrp2; *Abcc2*), Mrp4 (*Abcc4*), sodium phosphate co-transporter 1 (Npt1; *Slc17a1*) in rodents, and MRP2 (*ABCC2*), MRP4 (*ABCC4*), NPT1 (*SLC17A1*), hOAT4 (*SLC22A11*), and URAT1 (*SLC22A12*) in humans [9, 35, 36]. In addition to the ABC transporter, hOAT4 has been shown to mediate bidirectional transport of IS, suggesting that hOAT4 is partly involved in the apical efflux of IS in human proximal tubules [25]. These transporters are candidate transporters involved in secretion and/or reabsorption of uremic toxins. Further studies are necessary to identify transporters responsible for the luminal secretion of uremic toxins, and to investigate the interaction between uremic toxins and endogenous/exogenous organic anions via these transporters.

In patients of renal failure, pathophysiologic alterations may affect the activity of transporters. It has been suggested that the expression levels of some transporters are changed in a rat model of renal failure [23, 37, 38]. rOat1, hOAT1, and rOAT3 are considered to be organic anion/dicarboxylate exchangers indirectly coupled with a Na^+ -dicarboxylate cotransporter [7, 17, 39], thus, abnormalities in energy metabolism may also influence the transport activity in renal failure patients. Taking into consideration the fact that accumulation of uremic toxins, especially HA, attenuates the renal elimination via rOats/hOATs, plasma HA may serve as a criterion to evaluate the interaction of uremic toxins and drugs in patients suffering from uremic syndrome. In addition, a certain amount of uremic toxins is associated with plasma and urine specimens from healthy subjects [30], which enable us to obtain in vivo renal clearance and scaling

factors to extrapolate in vitro clearance to in vivo. Based on the RAF concept, uremic toxins, especially HA, IA, and CMPF, may be used as reference compounds to estimate roughly the renal clearance of organic anions and therefore, to avoid excessive accumulation of drugs in the body prior to treatment. Further clinical studies are necessary to validate the correlation between renal clearance of uremic toxins and drugs.

CONCLUSION

We have demonstrated that rOat1/hOAT1 and rOat3/hOAT3 are responsible for the renal uptake of uremic toxins on the basolateral membrane of the proximal tubules. Both rOat1 and rOat3 contribute to IS transport in the kidney. rOat1 is predominantly responsible for the renal uptake of IA and HA, while rOat3 plays a major role in the renal uptake of CMPF. Furthermore, rOat1/hOAT1 and rOat3/hOAT3 are potential sites of interaction between uremic toxins and endogenous or exogenous compounds. These findings may help us understand the pathophysiologic functions of the kidney as a detoxifying system and improve the treatment of uremic patients.

ACKNOWLEDGMENT

The authors would like to thank Sankyo (Tokyo, Japan) for kindly providing pravastatin. This study was performed through the Advanced and Innovational Research program in Life Sciences from the Ministry of Education, Culture, Sports, Science and Technology, the Japanese Government.

Reprint requests to Yuichi Sugiyama, Ph.D., Professor, Graduate School of Pharmaceutical Sciences, The University of Tokyo, 7-3-1, Hongo, Bunkyo-ku, Tokyo 113-0033, Japan.
E-mail: sugiyama@mol.f.u-tokyo.ac.jp

REFERENCES

1. VANHOLDER R, ARGILES A, BAURMEISTER U, et al: Uremic toxicity: Present state of the art. *Int J Artif Organs* 24:695–725, 2001
2. TSUTSUMI Y, DEGUCHI T, TAKANO M, et al: Renal disposition of a furan dicarboxylic acid and other uremic toxins in the rat. *J Pharmacol Exp Ther* 303:880–887, 2002
3. DZURIK R, SPUSTOVA V, KRIVOSIKOVA Z, GAZDIKOVA K: Hippurate participates in the correction of metabolic acidosis. *Kidney Int* 78(Suppl):S278–281, 2001
4. NIWA T: Organic acids and the uremic syndrome: Protein metabolite hypothesis in the progression of chronic renal failure. *Semin Nephrol* 16:167–182, 1996
5. MIYAZAKI T, ISE M, SEO H, NIWA T: Indoxyl sulfate increases the gene expressions of TGF-beta 1, TIMP-1 and pro-alpha 1(I) collagen in uremic rat kidneys. *Kidney Int* 62(Suppl):S15–22, 1997
6. MIYAZAKI T, AOYAMA I, ISE M, et al: An oral sorbent reduces overload of indoxyl sulphate and gene expression of TGF-beta1 in uraemic rat kidneys. *Nephrol Dial Transplant* 15:1773–1781, 2000
7. SEKINE T, WATANABE N, HOSOYAMADA M, et al: Expression cloning and characterization of a novel multispecific organic anion transporter. *J Biol Chem* 272:18526–18529, 1997
8. TOJO A, SEKINE T, NAKAJIMA N, et al: Immunohistochemical localization of multispecific renal organic anion transporter 1 in rat kidney. *J Am Soc Nephrol* 10:464–471, 1999

9. KUSUHARA H, SUGIYAMA Y: Role of transporters in the tissue-selective distribution and elimination of drugs: Transporters in the liver, small intestine, brain and kidney. *J Control Release* 78:43–54, 2002
10. SEKINE T, CHA SH, TSUDA M, et al: Identification of multispecific organic anion transporter 2 expressed predominantly in the liver. *FEBS Lett* 429:179–182, 1998
11. KUSUHARA H, SEKINE T, UTSUNOMIYA-TATE N, et al: Molecular cloning and characterization of a new multispecific organic anion transporter from rat brain. *J Biol Chem* 274:13675–13680, 1999
12. BUIST SC, CHERRINGTON NJ, CHOUDHURI S, et al: Gender-specific and developmental influences on the expression of rat organic anion transporters. *J Pharmacol Exp Ther* 301:145–151, 2002
13. KOJIMA R, SEKINE T, KAWACHI M, et al: Immunolocalization of multispecific organic anion transporters, OAT1, OAT2, and OAT3, in rat kidney. *J Am Soc Nephrol* 13:848–857, 2002
14. HASEGAWA M, KUSUHARA H, SUGIYAMA D, et al: Functional involvement of rat organic anion transporter 3 (rOat3; Slc22a8) in the renal uptake of organic anions. *J Pharmacol Exp Ther* 300:746–753, 2002
15. SUGIYAMA D, KUSUHARA H, SHITARA Y, et al: Characterization of the efflux transport of 17beta-estradiol-D-17beta-glucuronide from the brain across the blood-brain barrier. *J Pharmacol Exp Ther* 298:316–322, 2001
16. HASEGAWA M, KUSUHARA H, ENDOU H, SUGIYAMA Y: Contribution of organic anion transporters to the renal uptake of anionic compounds and nucleoside derivatives in rat. *J Pharmacol Exp Ther* 305:1087–1097, 2003
17. HOSOYAMADA M, SEKINE T, KANAI Y, ENDOU H: Molecular cloning and functional expression of a multispecific organic anion transporter from human kidney. *Am J Physiol* 276:F122–128, 1999
18. CHA SH, SEKINE T, FUKUSHIMA JI, et al: Identification and characterization of human organic anion transporter 3 expressing predominantly in the kidney. *Mol Pharmacol* 59:1277–1286, 2001
19. MOTOHASHI H, SAKURAI Y, SAITO H, et al: Gene expression levels and immunolocalization of organic ion transporters in the human kidney. *J Am Soc Nephrol* 13:866–874, 2002
20. BOUMENDIL-PODEVIN EF, PODEVIN RA, RICHEL G: Uricosuric agents in uremic sera. Identification of indoxyl sulfate and hippuric acid. *J Clin Invest* 55:1142–1152, 1975
21. COSTIGAN MG, LINDUP WE: Plasma clearance in the rat of a furan dicarboxylic acid which accumulates in uremia. *Kidney Int* 49:634–638, 1996
22. DEGUCHI T, OHTSUKI S, OTAGIRI M, et al: Major role of organic anion transporter 3 in the transport of indoxyl sulfate in the kidney. *Kidney Int* 61:1760–1768, 2002
23. ENOMOTO A, TAKEDA M, TOJO A, et al: Role of organic anion transporters in the tubular transport of indoxyl sulfate and the induction of its nephrotoxicity. *J Am Soc Nephrol* 13:1711–1720, 2002
24. MOTOJIMA M, HOSOKAWA A, YAMATO H, et al: Uraemic toxins induce proximal tubular injury via organic anion transporter 1-mediated uptake. *Br J Pharmacol* 135:555–563, 2002
25. ENOMOTO A, TAKEDA M, TAKI K, et al: Interactions of human organic anion as well as cation transporters with indoxyl sulfate. *Eur J Pharmacol* 466:13–20, 2003
26. TSUTSUMI Y, MARUYAMA T, TAKADATE A, et al: Interaction between two dicarboxylate endogenous substances, bilirubin and an uremic toxin, 3-carboxy-4-methyl-5-propyl-2-furanpropanoic acid, on human serum albumin. *Pharm Res* 16:916–923, 1999
27. YAMAOKA K, TANIGAWARA Y, NAKAGAWA T, UNO T: A pharmacokinetic analysis program (multi) for microcomputer. *J Pharmacobio-dyn* 4:879–885, 1981
28. CRESPI C: Xenobiotics-metabolizing human cells as tools for pharmacological and toxicological research. *Adv Drug Res* 26:179–235, 1995
29. NAGATA Y, KUSUHARA H, ENDOU H, SUGIYAMA Y: Expression and functional characterization of rat organic anion transporter 3 (rOat3) in the choroid plexus. *Mol Pharmacol* 61:982–988, 2002
30. SAKAI T, MARUYAMA T, IMAMURA H, et al: Mechanism of stereoselective serum binding of ketoprofen after hemodialysis. *J Pharmacol Exp Ther* 278:786–792, 1996
31. VANOLDEN RW, ACKER BA, KOOMEN GC, et al: Contribution of tubular anion and cation secretion to residual renal function in chronic dialysis patients. *Clin Nephrol* 49:167–172, 1998
32. LIM CF, BERNARD BF, JONG M, et al: A furan fatty acid and indoxyl sulfate are the putative inhibitors of thyroxine hepatocyte transport in uremia. *J Clin Endocrinol Metab* 76:318–324, 1993
33. NIWA T, AOYAMA I, TAKAYAMA F, et al: Urinary indoxyl sulfate is a clinical factor that affects the progression of renal failure. *Miner Electrolyte Metab* 25:118–122, 1999
34. ILIC S, RAJIC M, VLAJKOVIC M, et al: The predictive value of 131I-hippurate clearance in the prognosis of acute renal failure. *Ren Fail* 22:581–589, 2000
35. ENOMOTO A, KIMURA H, CHAIROUNGDUA A, et al: Molecular identification of a renal urate anion exchanger that regulates blood urate levels. *Nature* 417:447–452, 2002
36. AUBEL RA, SMEETS PH, PETERS JG, et al: The MRP4/ABCC4 gene encodes a novel apical organic anion transporter in human kidney proximal tubules: Putative efflux pump for urinary cAMP and cGMP. *J Am Soc Nephrol* 13:595–603, 2002
37. LAOUARI D, YANG R, VEAU C, et al: Two apical multidrug transporters, P-gp and MRP2, are differently altered in chronic renal failure. *Am J Physiol Renal Physiol* 280:F636–645, 2001
38. JI L, MASUDA S, SAITO H, INUI K: Down-regulation of rat organic cation transporter rOCT2 by 5/6 nephrectomy. *Kidney Int* 62:514–524, 2002
39. SWEET DH, CHAN LM, WALDEN R, et al: Organic anion transporter 3 (Slc22a8) is a dicarboxylate exchanger indirectly coupled to the Na⁺ gradient. *Am J Physiol Renal Physiol* 284:F763–769, 2003

Pharmacokinetics and Tissue Distribution of Uraemic Indoxyl Sulphate in Rats

Tsuneo Deguchi, Mikio Nakamura, Yasuhiro Tsutsumi, Ayaka Suenaga and Masaki Otagiri*

Graduate School of Pharmaceutical Sciences, Kumamoto University, 5-1 Oe-honmachi, Kumamoto 862-0973, Japan

ABSTRACT: The purpose of the present study was to examine the pharmacokinetic properties of indoxyl sulphate, a harmful uraemic toxin that accumulates during chronic renal failure. The pharmacokinetics and tissue distribution of indoxyl sulphate were examined in normal and 5/6 nephrectomized (CRF) rats. The uptake process of indoxyl sulphate by rat renal cortical slices *in vitro* was also investigated. Endogenous indoxyl sulphate was found to be mainly distributed in the kidney. The rate of elimination of indoxyl sulphate from plasma was lower in CRF rats compared with sham-operated rats. The majority of intact indoxyl sulphate was excreted in the urine. In renal cortical slice experiments, uptake of indoxyl sulphate was a saturable process with a K_m of 43.0 μM . Furthermore, sulphate conjugates, such as oestrone sulphate and dehydroepiandrosterone sulphate, inhibited the uptake of indoxyl sulphate to a greater extent than PAH. Thus, indoxyl sulphate is primarily eliminated from the plasma via the kidney by active tubular secretion, and renal uptake of indoxyl sulphate appears to be mediated by an organic anion transport system with a high affinity for oestrone sulphate and dehydroepiandrosterone sulphate. Copyright © 2003 John Wiley & Sons, Ltd.

Abbreviations used: CRF, chronic renal failure; IA, indoleacetic acid; OAT, organic anion transporter; PAH, *p*-aminohippuric acid; DHEAS, dehydroepiandrosterone sulphate; HSA human serum albumin

Key words: indoxyl sulphate; uraemic toxin; chronic renal failure; organic anion transporter

Introduction

Serum levels of the uraemic toxin indoxyl sulphate are markedly elevated in patients with uraemia [1,2]. The accumulation of this toxin in serum causes a number of pathological effects, such as the inhibition of drug binding to serum albumin [3–5], irregularities in thyroid function [6] and inhibition of active tubular secretion [7–9]. Indoxyl sulphate is particularly known to be the circulating substance that stimulates the progression of chronic renal failure [7, 8]. The

oral administration of indoxyl sulphate to uraemic rats stimulates the progression of glomerular sclerosis and results in impaired renal function [8]. Therefore, indoxyl sulphate can be classified as a harmful uraemic toxin [10].

Despite the importance of the role played by indoxyl sulphate in the pathophysiology of uraemia, little information is available regarding its pharmacokinetics in animals, and no studies on its tissue distribution have been reported. Indoxyl sulphate is synthesized in the liver from indole through indoxyl. Indole is produced from tryptophan by intestinal bacteria such as *Escherichia coli* [11, 12]. Indoxyl sulphate is thought to be excreted mainly via the kidney because excretion via the urine is inefficient in uraemic

*Corresponding to: Graduate School of Pharmaceutical Sciences, Kumamoto University, 5-1 Oe-honmachi, Kumamoto 862-0973, Japan. E-mail: otagirim@gpo.kumamoto-u.ac.jp

patients, and thus indoxyl sulphate accumulates in the body [2, 7]. The glomerular filtration of indoxyl sulphate is considered to be minimal, because more than 96% is bound to albumin [13]. Indoxyl sulphate significantly inhibits the uptake of *p*-aminohippuric acid (PAH) by isolated renal tubules [9] and reduces renal clearance of PAH [7, 8]. Therefore, excretion of indoxyl sulphate via the urine is primarily thought to be via tubular secretion, presumably by an organic anion transport system [9].

To clarify the pharmacological properties of indoxyl sulphate, an analysis of the nephrotoxicity and uraemic symptoms it induces is needed. The distribution and accumulation of indoxyl sulphate in various tissues could be an important step in the expression of uraemic toxicity in renal failure. Furthermore, the inhibition of transporters by indoxyl sulphate would lead to the inhibition of active tubular secretion of many other exogenous and endogenous organic acids that are transported by the same system. This inhibition may extend to other sites of organic acid transport, such as those in the brain and liver, and may induce numerous uraemic symptoms.

To begin developing an understanding of the mechanisms of uraemic symptoms and the pharmacological action of indoxyl sulphate, a pharmacokinetic investigation was conducted following a single i.v. administration to normal and 5/6 nephrectomized rats. Renal and biliary excretion of indoxyl sulphate after i.v. administration to anaesthetized rats, as well as tissue distribution of endogenous indoxyl sulphate, were studied. Moreover, indoxyl sulphate uptake by renal cortical slices *in vitro* was investigated in order to determine whether an organic anion transporter is involved in the renal excretion of indoxyl sulphate.

Materials and Methods

Materials

HSA was donated by the Chemo-Sera-Therapeutic Research Institute (Kumamoto, Japan). HSA was defatted by treatment with activated charcoal in solution at 0°C, acidified with H₂SO₄ to

pH 3 and then lyophilized. The HSA used in this study showed only one band of approximately 66 kDa by SDS-PAGE. Indoxyl sulphate, probenecid, oestrone sulphate, dehydroepiandrosterone sulphate (DHEAS), valproic acid and digoxin were obtained from Sigma Chemical Co. (St Louis, MO, USA). *p*-Aminohippuric acid (PAH), bromosulphophthalein, indoleacetic acid (IA) and salicylic acid were obtained from Nacalai Tesque (Kyoto, Japan). Benzylpenicillin potassium salt, cimetidine, indomethacin, taurocholic acid and tetraethylammonium were obtained from Wako Pure Chemical Industries Ltd (Osaka, Japan). All chemicals were analytical grade.

Induction of CRF by surgical reduction of renal mass

Experimental CRF was induced using the so-called 5/6 nephrectomized model by the excision of about two-thirds of the left kidney and total right nephrectomy (chronic renal failure model; CRF). Rats were anaesthetized with sodium pentobarbital (60 mg/kg) by intraperitoneal injection and during surgery, the body temperature of the rats was maintained by a warming lamp. The left kidney was exposed through a left flank incision, gently dissected free from the adrenal gland, and the upper and lower poles were excised. One week later, rats were again anaesthetized with sodium pentobarbital, and the right kidney was removed through a right flank incision after being dissected free of the adrenal gland. A control group of rats was subjected to sham operations identical to those used for CRF rats, except that the kidney or poles of the kidney were not removed. Sham-operated rats were monitored for 2 weeks in parallel with 5/6 nephrectomized rats. Two weeks following the induction of 5/6 nephrectomy, CRF rats with severe chronic renal insufficiency were selected based on their serum creatinine (>1.4 mg/dl) and BUN (>2.5 mg/dl) level.

Tissue distribution of indoxyl sulphate

The brain, heart, lung, liver, spleen, kidney and testis were removed and weighed, after killing the sham-operated rats and CRF rats by decapitation. A sample (0.5 g) of each tissue was homogenized in 5 ml of 1M KH₂PO₄. A 50 µl

aliquot of this solution was added directly to 100 µl of acetonitrile and an aliquot of a stock solution of IA was added as an internal standard. After centrifugation at $3000 \times g$ for 10 min, the supernatant was assayed by HPLC.

The distribution of indoxyl sulphate in each tissue was expressed as the C_t/C_p ratio (concentration of indoxyl sulphate per gram of each tissue divided by the concentration of indoxyl sulphate in plasma).

Pharmacokinetics of indoxyl sulphate in anaesthetized rat

Male Wistar rats (250–290 g; bred and maintained in the department animal facility) were anaesthetized with sodium pentobarbital (60 mg/kg) by intraperitoneal injection, and the left femoral vein and artery were subsequently cannulated.

Indoxyl sulphate was administered at a dose of 46.9 µmol/kg (10 mg/kg) by rapid infusion into the femoral vein. After each infusion the cannulae were flushed with a small volume of heparinized saline in order to ensure the complete administration of each dose and to prevent clot formation.

Blood samples (200 µl) were taken from the femoral artery at 1, 3, 6, 15, 30, 60, 90, 120 and 180 min. Blood was placed in graduated microcentrifuge tubes (0.6 ml) that contained a drop of heparinized saline to serve as an anticoagulant. Blood samples were centrifuged ($3000 \times g$ for 10 min) and plasma was removed. An aliquot (50 µl) of plasma was added directly to 100 µl of acetonitrile and indoxyl sulphate was extracted using the procedure described above. The plasma concentration of indoxyl sulphate was estimated by subtracting the concentration of endogenous indoxyl sulphate from that detected in the samples.

Urinary and biliary excretion

Male Wistar rats (250–290 g; bred and maintained in the departmental animal facility) underwent a surgical procedure under light anaesthesia with phenobarbital where cannulae were inserted into the femoral vein and artery using polyethylene tubing (polyethylene-50: i.d., 0.58 mm; o.d., 0.9655 mm; Becton Dickson & Co., Parsippany, NJ). The bile duct was also cannulated with

polyethylene tubing (polyethylene-10: i.d., 0.28 mm; o.d., 0.61 mm), as was the bladder (polyethylene-8: o.d., 2.33 mm; Hibiki Co., Tokyo, Japan). The body temperature of the rats was maintained by a warming lamp. Thirty minutes before i.v. injection, control samples of bile and urine were collected. Bile and urine were collected at 0–30, 30–60, 60–90, 90–120, 120–150 and 150–180 min post injection.

Determination of the free (unbound) concentration of uraemic toxins

Serum concentrations of free indoxyl sulphate were estimated by ultrafiltration as previously described [14]. Free fractions of indoxyl sulphate was determined according to the following equation:

$$f = \frac{C_{\text{free}}}{C_{\text{total}}} \times 100 (\%) \quad (1)$$

where f represents the free fraction of indoxyl sulphate, C_{free} the free concentration and C_{total} the total concentration of indoxyl sulphate.

Uptake by rat renal cortical slices

The uptake of indoxyl sulphate by rat renal cortical slices was investigated using a procedure described in the literature [15]. The rats were anaesthetized and the kidneys promptly removed, decapsulated and placed in an ice-cold oxygenated rinse medium, which consisted of 97 mM NaCl, 40 mM KCl, 0.74 mM $\text{CaCl}_2 \cdot 2\text{H}_2\text{O}$ and 7.5 mM sodium phosphate-chloride buffer, at pH 7.4. Renal cortical slices (weight 10–20 mg/slice; about 0.5 mm in thickness) were cut free-hand with Gillette valet strip blades about 7.60 cm (3 in) long (Sabre International Products Ltd., Reading, UK). Two cortical slices were prepared from each half-kidney and were stored on ice in oxygenated rinse medium for no longer than 15 min prior to incubation. Two slices were placed in each flask and the medium (consisting of rinse medium, 10 mM L-lactate and 10 mM L-pyruvate) was thoroughly gassed with 100% oxygen for about 1 min both before and after the addition of the slices. The flasks were then tightly sealed with rubber stoppers and incubated at 25°C in a shaking water bath at 60 cycles/min for 60 min. After incubation, the

flasks were placed on ice, and the slices were promptly removed, gently blotted and weighed. Tissue blanks were prepared by omitting indoxyl sulphate from the incubation medium.

Uptake of indoxyl sulphate was expressed as the S/M ratio (i.e. the concentration of indoxyl sulphate per gram of kidney tissue divided by the concentration of indoxyl sulphate per milliliter of medium). The active uptake velocity was calculated by subtracting the uptake velocity at 4°C (non-specific uptake) from that at 25°C.

HPLC conditions

The HPLC system consisted of a Hitachi L-6000 intelligent pump and a Hitachi F-1050 fluorescence spectrophotometer. A column of LiChrosorb RP-18 (Cica Merck, Tokyo, Japan) was used as the stationary phase. The mobile phase consisted of acetate buffer (0.2 M, pH 4.5)-acetonitrile (83:17 v/v). The flow rate was 1.0 ml/min. Indoxyl sulphate and IA were detected by means of a fluorescence monitor. Excitation/emission wavelengths were 280/375 nm for indoxyl sulphate and IA. The coefficients of variation for the HPLC methods were similar (< 5%).

Data and statistical analysis

Plasma concentration profiles were analysed by fitting the following biexponential equation according to the nonlinear least-squares method (MULTI) [16]:

$$C_p = A \cdot \exp(-\alpha t) + B \cdot \exp(-\beta t) \quad (2)$$

Parameters of pharmacokinetics were calculated using the following equations:

$$AUC_{0 \rightarrow \infty} = \frac{A}{\alpha} + \frac{B}{\beta} \quad (3)$$

$$CL_{tot} = \frac{\text{Dose}}{AUC_{0 \rightarrow \infty}} \quad (4)$$

$$t_{1/2\beta} = \frac{0.693}{\beta} \quad (5)$$

$$V_1 = \frac{\text{Dose}}{A + B} \quad (6)$$

$$C_0 = \frac{\text{Dose}}{V_1} \quad (7)$$

$$CL_{urinary} = \frac{X_{urine0 \rightarrow 180 \text{ min}}}{AUC_{0 \rightarrow 180 \text{ min}}} \quad (8)$$

$$CL_{biliary} = \frac{X_{bile0 \rightarrow 180 \text{ min}}}{AUC_{0 \rightarrow 180 \text{ min}}} \quad (9)$$

where $AUC_{0 \rightarrow \infty}$, CL_{tot} , $t_{1/2\beta}$, V_1 , $CL_{urinary}$, $X_{urine0 \rightarrow 180 \text{ min}}$, $AUC_{0 \rightarrow 180 \text{ min}}$, $CL_{biliary}$ and $X_{bile0 \rightarrow 180 \text{ min}}$ represent the AUC from zero to infinity, total body clearance, β phase half-life, distribution volume of central compartment, urinary clearance, amount of cumulative indoxyl sulphate in the urine, AUC from zero to 180 min, biliary clearance and the cumulative amount of cumulative indoxyl sulphate in the bile, respectively.

In the renal cortical slice uptake study, kinetic parameters were obtained using the following equation:

$$v = \frac{V_{max} \times S}{K_m + S} \quad (10)$$

where v is the velocity of the renal uptake of indoxyl sulphate (nmol/min/g kidney), S the indoxyl sulphate concentration in the medium (μM), K_m the Michaelis-Menten constant (μM), and V_{max} the maximum uptake rate (nmol/min/g kidney). Fitting was performed by the nonlinear least-squares method using the MULTI program and the Damping Gauss Newton method algorithm was used for fitting.

All data are presented as the mean \pm SEM, and n refers to the number of animals used in each experiment. The Student's t -test was used to analyse differences between two groups. ANOVA was used to analyse differences between more than two groups, and the degree of significance between two means in these groups was evaluated using the modified Fisher's least squares difference method.

Results

Authentic indoxyl sulphate was recovered from rat plasma in a yield of over 95% in each case. Sham-operated and 5/6 nephrectomized (CRF) rat plasma contained a substance that had chromatographic characteristics identical to indoxyl sulphate. Mean (\pm SEM) endogenous con-

centrations of this substance were 7.60 ± 1.08 and $46.6 \pm 1.59 \mu\text{M}$, respectively ($n = 3$).

Pharmacokinetic properties of indoxyl sulphate

To clarify the mechanism by which indoxyl sulphate accumulates, the pharmacokinetic properties were examined using normal and CRF rats.

Figure 1 shows the tissue distribution of indoxyl sulphate in the control and CRF rats. These results indicate that indoxyl sulphate was

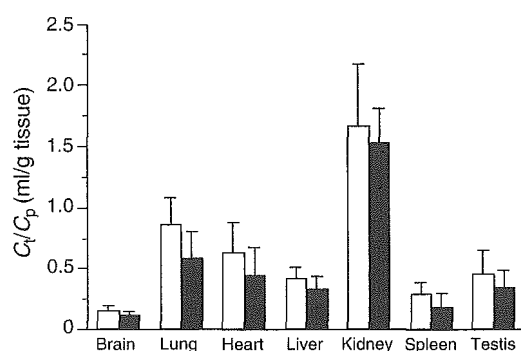


Figure 1. Tissue distribution of indoxyl sulphate in sham and CRF rats. Endogenous indoxyl sulphate was measured in various tissues of sham (open bars) and CRF rats (closed bars). Distribution of indoxyl sulphate in each tissue is expressed as C_t/C_p ratio, i.e. the concentration of indoxyl sulphate per gram of each tissue divided by concentration of indoxyl sulphate in plasma (sham rats; $7.60 \pm 1.08 \mu\text{M}$, CRF rats; $46.6 \pm 1.59 \mu\text{M}$). Each bar represents the mean \pm SEM of three different experiments

present in the highest concentration in the kidney. The concentration of indoxyl sulphate in the kidney of control and CRF rats was 12.6 ± 2.7 and $71.2 \pm 8.9 \text{ nmol/g}$, respectively.

Figure 2A shows the plasma-time concentration profiles for indoxyl sulphate after administration of $46.9 \mu\text{mol/kg}$ to the control and CRF rats. The plasma clearance of indoxyl sulphate was significantly decreased in CRF rats (Table 1). The biological half-life ($t_{1/2\beta}$) was more prolonged in CRF rats ($526 \pm 40 \text{ min}$) than in the control rats ($59.1 \pm 6.2 \text{ min}$). Indoxyl sulphate has a high affinity for albumin (the percentage bound was about 97.1%) and binding to normal rat serum was maintained at concentrations of indoxyl sulphate up to $600 \mu\text{M}$ (data not shown). Furthermore, the distribution volume of indoxyl sulphate was unchanged in the CRF rats compared with the control rats (Table 1). Considering these observations, the serum protein binding of indoxyl sulphate to serum proteins would not be saturated under these experimental conditions.

To investigate further, the urinary and biliary excretion of indoxyl sulphate was also examined (Figure 2B, Table 1). In the control rats, the renal (CL_{urinary}) and biliary (CL_{biliary}) clearances of indoxyl sulphate were determined to be 2.42 ± 0.02 and $0.0002 \pm 0.0001 \text{ ml/min/kg}$, respectively. The majority of indoxyl sulphate was excreted in an unaltered state and the main route was via the urine. Furthermore, urinary indoxyl

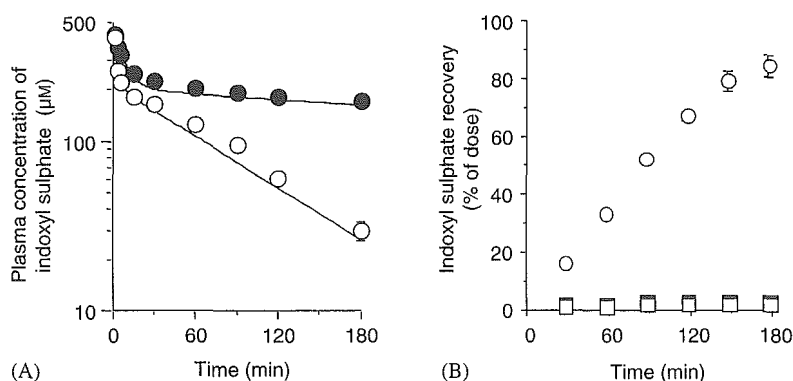


Figure 2. Disposition profiles after i.v. administration of indoxyl sulphate in sham and CRF rats. (A) Indoxyl sulphate was administered at $46.9 \mu\text{mol/kg}$ by rapid infusion into the femoral vein in sham (○) and CRF rats (●). (B) Bile (sham, □; CRF, ■) and urine (sham, ○; CRF, not detected) were collected at 30, 60, 90, 120, 150 and 180 min post injection (10 mg/kg). See Materials and Methods for experimental details. Each point represents the mean \pm SEM of four different experiments

Table 1. Pharmacokinetic parameters for indoxyl sulphate after i.v. administration (46.9 µmol/kg) to sham and CRF rats

Parameter	Sham rats	CRF rats
AUC (µmol/ml min)	19.2 ± 0.7	114 ± 4a
CL _{tot} (ml/min/kg)	2.45 ± 0.08	0.30 ± 0.01a
t _{1/2β} (min)	59.1 ± 6.2	526 ± 40a
V ₁ (ml/kg)	90.1 ± 5.1	95.6 ± 5.3
CL _{urinary} (ml/min/kg)	2.42 ± 0.02	ND
CL _{biliary} (ml/min/kg)	0.002 ± 0.0001	0.005 ± 0.0002

Each value represents the mean ± SEM (n = 4).

^ap < 0.001, significantly different from the corresponding parameter in sham operated rats. ND, not detected.

Table 2. Dose dependent pharmacokinetics for indoxyl sulphate after i.v. administration

Parameter	Dose		
	23.5 µmol/kg	46.9 µmol/kg	235 µmol/kg
AUC (µmol/ml min)	2.88 ± 0.06	16.3 ± 0.7	67.3 ± 1.3
CL _{tot} (ml/min/kg)	6.83 ± 0.70	2.87 ± 0.09	2.68 ± 0.09
t _{1/2β} (min)	23.5 ± 0.4	57.8 ± 17.0	75.2 ± 2.4
V ₁ (ml/kg)	89.3 ± 2.1	88.3 ± 6.1	150 ± 6
C ₀ (µM)	263 ± 6	530 ± 38	1562 ± 61

Each value represents the mean ± SEM (n = 4).

sulphate was not detected in the CRF rats, and no changes in CL_{biliary} were observed. These results (Figures 1 and 2) indicate that the main elimination pathway of indoxyl sulphate is via renal excretion.

The glomerular filtration of indoxyl sulphate is likely to be minimal, due to its high affinity for albumin. The dose dependency of indoxyl sulphate pharmacokinetic parameters after i.v. administration was also examined (Table 2). Plasma clearance decreased with increasing dosage from 23.5 to 235 µmol/kg (saturation), suggesting that renal tubular secretion is responsible for the elimination of indoxyl sulphate. The coadministration of *p*-aminohippuric acid (PAH) (1 mmol/kg) or probenecid (175 µmol/kg), typical substrates/inhibitors of the organic anion transport system in the kidney, also decreased the plasma and urinary clearance of indoxyl sulphate (Table 3). These results suggest that carrier-mediated transport, probably an organic anion transporter, is involved in the excretion of indoxyl sulphate in the kidney.

Table 3. Pharmacokinetic parameters for indoxyl sulphate after i.v. administration (46.9 µmol/kg) of indoxyl sulphate alone, and indoxyl sulphate with PAH (1 mmol/kg) or probenecid (175 µmol/kg)

Parameter	Control	With PAH	With probenecid
AUC (µmol/ml min)	16.3 ± 0.7	36.0 ± 0.3b	74.5 ± 1.7b
CL _{tot} (ml/min/kg)	2.87 ± 0.09	1.26 ± 0.03b	0.57 ± 0.03b
t _{1/2β} (min)	57.8 ± 17.0	89.2 ± 3.5a	189 ± 2b
V ₁ (ml/kg)	88.3 ± 6.1	96.4 ± 4.4	91.5 ± 1.9
CL _{urinary} (ml/min/kg)	2.42 ± 0.02	1.01 ± 0.01b	0.25 ± 0.01b

Each value represents the mean ± SEM (n = 4).

^ap < 0.01, ^bp < 0.001, significantly different from corresponding control parameter.

Mechanism of uptake of indoxyl sulphate by renal cortical slices

The uptake of indoxyl sulphate by renal cortical slices was examined. At 25°C, the slice-to-medium ratio (S/M) was 8.20 ± 0.14 ml/h/g kidney (n = 3), whereas under anaerobic conditions at 4°C, this value was 1.49 ± 0.18 ml/h/g kidney (n = 3). These results suggest that active transport is involved in the uptake of indoxyl sulphate by renal cortical slices and provides further support for the above *in vivo* data. The active uptake of indoxyl sulphate by renal cortical slices was linear for at least 20 min (data not shown). To estimate the K_m and V_{max} values for the active uptake of indoxyl sulphate from the initial rate, the uptake velocity of indoxyl sulphate was measured over a range of concentrations (10–800 µM) after incubation for 20 min at 25°C in three separate experiments (Figure 3A and B). Nonspecific uptake, measured at 4°C, was subtracted from the uptake at 25°C. The mean K_m and V_{max} values for active uptake of indoxyl sulphate were 43.0 ± 7.8 µM and 16.8 ± 1.4 nmol/min/g kidney, respectively. In addition, a kinetic analysis of the renal uptake of indoxyl sulphate in the presence of 5% human serum albumin (HSA) was performed. The uptake by renal cortical slices was measured at total concentrations between 30 µM and 10 mM indoxyl sulphate for 20 min at 25°C (Figure 3C and D). The mean K_m and V_{max} values for the active uptake of indoxyl sulphate in the presence of 5% HSA were 505 ± 45 µM and 17.6 ± 1.4 nmol/min/g kidney, respectively. Consider-

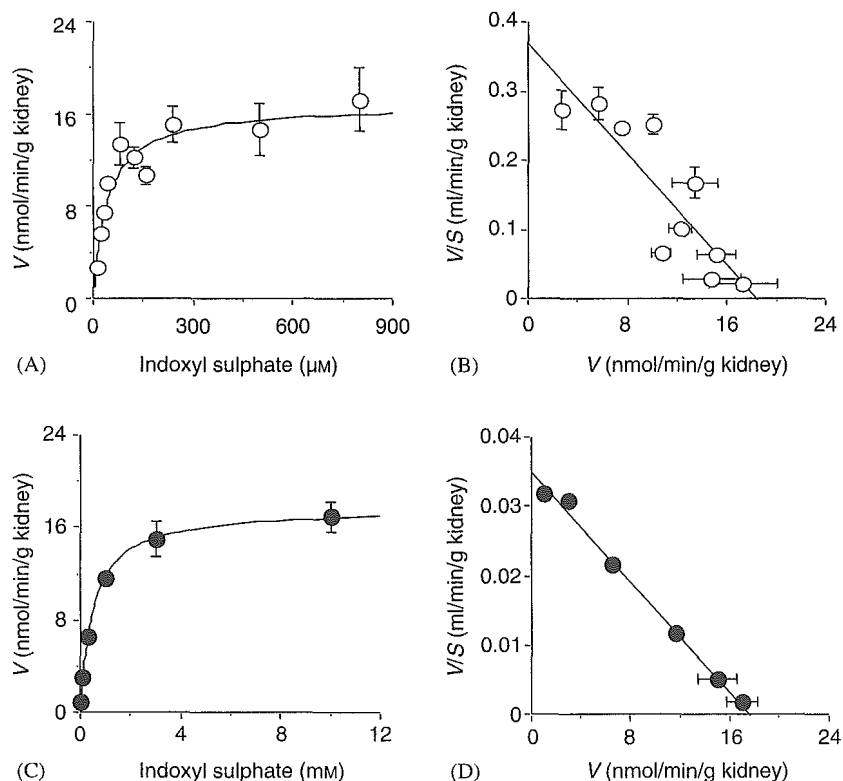


Figure 3. Concentration-dependence of indoxyl sulphate uptake by renal cortical slices. The uptake of indoxyl sulphate by renal cortical slices was measured over a 20 min period at 25°C. The active uptake velocity was calculated by subtracting the uptake velocity in the 4°C (non-specific uptake) from that at the 25°C. Experiments were performed in the absence (A,B) or presence (C,D) of 5% human serum albumin (HSA). An Eadie-Hofstee plot analysis was performed for each experiment (B,D). Each point represents the mean \pm SEM of three to seven different experiments

ing this result, the findings of the *in vivo* study (Table 2) are likely caused by saturation of the renal uptake of indoxyl sulphate.

Inhibition by PAH or probenecid in renal excretion during the *in vivo* experiments suggest that the same mechanism is involved in the renal uptake of indoxyl sulphate. In order to confirm whether the uptake of indoxyl sulphate is mediated by the organic anion transport system, the effect of various compounds on indoxyl sulphate uptake by rat renal cortical slices was examined. As shown in Figure 4, the uptake of indoxyl sulphate by renal cortical slices was inhibited by both probenecid and PAH, which was consistent with the findings of the *in vivo* study (Table 3). This indicates that an organic anion transport system is involved in the uptake of indoxyl sulphate in the kidney. Furthermore,

dehydroepiandrosterone sulphate (DHEAS), oestrone sulphate, bromosulphophthalein, benzylpenicillin, cimetidine and indomethacin also inhibited the uptake of indoxyl sulphate, while salicylic acid, valproic acid, digoxin, taurocholic acid and tetraethylammonium had little or no inhibitory effect. Sulphate conjugates oestrone sulphate and DHEAS particularly showed stronger inhibitory effects than PAH.

To estimate the inhibitory effect of PAH, oestrone sulphate and DHEAS on the uptake of indoxyl sulphate in the kidney, the apparent inhibitory constant (K_i) of these anions for inhibiting indoxyl sulphate uptake was calculated using a Dixon plot. The K_i values for oestrone sulphate ($25.1 \pm 5.0 \mu\text{M}$) and DHEAS ($15.8 \pm 2.4 \mu\text{M}$) were smaller than the value for PAH ($115 \pm 12 \mu\text{M}$). These results suggest that in